SUPPLEMENT 1

HONG KONG MEDICAL JOURNAL 香港醫學雜誌 31(S1)

HONG KONG

Volume 31 Number 1 **February 2025**

MEDICAL JOURNAL
香港醫學雜誌

The official publication of the
Hong Kong Academy of Medicine and
the Hong Kong Medical Association

Health and Medical Research Fund
Research Dissemination Reports

醫療衞生研究基金
研究成果報告

Advanced technology
先進科技

Chinese medicine
中醫藥

Digital health
數位健康

Non-communicable diseases
非傳染病

Reproductive medicine
生殖醫學

Volume 31 Number 1 **February 2025**

Supplement 1

ISSN 1024-2708

香港醫學專科學院出版社
HONG KONG ACADEMY OF MEDICINE PRESS

HONG KONG MEDICAL JOURNAL 香港醫學雜誌
Volume 31 Number 1 **February 2025**
SUPPLEMENT 1

Health and Medical Research Fund

Research Dissemination Reports

DIGITAL HEALTH

NON-COMMUNICABLE DISEASES

REPRODUCTIVE MEDICINE

Editorial

Dissemination reports are concise informative reports of health-related research supported by the Health and Medical Research Fund administered by the Health Bureau. In this edition, we present 11 dissemination reports of projects related to advanced technology, Chinese medicine, digital health, non-communicable diseases, and reproductive medicine. In particular, research findings of three projects may provide insights to enhance clinical practices and help inform health policy formulation in Hong Kong.

Recurrence of hepatocellular carcinoma (HCC) within 2 years of curative surgery is common. HCC is usually diagnosed with computed tomography (CT) or magnetic resonance imaging. Lee et al[1] developed a deep-learning model using preoperative CT images to predict HCC recurrence after curative surgery. The model was trained using CT scans from 536 consecutive adult Chinese patients undergoing hepatic resection for histologically confirmed HCC. Internal and external validity testing was conducted using images from 135 and 560 patients, respectively. The final model, termed Recurr-NET, demonstrated superior risk stratification, compared with histological microvascular invasion, in predicting early and late HCC recurrence and mortality within 5 years.

Diabetic kidney disease (DKD) is the major cause of end-stage kidney failure leading to dialysis or transplantation and is characterised by progressively increasing albuminuria and/or declining renal function. DKD is conventionally treated by controlling blood pressure, blood glucose, and proteinuria. Some forms of traditional Chinese medicine (TCM) have been found to reduce the risk of end-stage kidney failure, but their effectiveness for DKD remains unclear. Chan et al[2] evaluated the effect of a 48-week course of add-on astragalus-based TCM, compared to usual care, among 118 Chinese DKD patients aged 35 to 80 years with stage 2 to 3 chronic kidney disease and macroalbuminuria. The results showed that the add-on TCM treatment significantly improved kidney function (ie, estimated glomerular filtration rate) and significantly lowered systolic blood pressure and gamma-glutamyl transferase levels (although not clinically significant) in these patients.

Knee osteoarthritis (OA) leads to reduced physical fitness, quality of life, and increased healthcare utilisation. Acupuncture has been shown to be an effective treatment for knee OA pain. Acupressure is a non-invasive variant of acupuncture in which fingers, hands, and elbows are used to stimulate the same acupoints. Yeung et al[3] conducted a randomised controlled trial of 314 middle-aged and older Chinese adults to evaluate the short- and medium-term effects of a 12-week course of self-administered acupressure, compared with knee health education, on alleviating knee OA pain. The results showed that two 2-hour sessions of self-administered acupressure training were effective in alleviating knee pain and improving mobility in older adults with knee OA. Participants in self-administered acupressure reported significantly lower pain scores at weeks 4, 8, and 12, compared with participants receiving knee health education. The self-administered acupressure training programme showed high acceptability and compliance and was cost-effective.

Supplement editors

Dr Anne Fung
Head
Research and Data Analytics Office
Health Bureau

Dr Richard A Collins
Senior Scientific Reviewer
Research and Data Analytics Office
Health Bureau

References

1. Lee EYP, Kuo M, Ng KCK, et al. Prediction of recurrence and survival using big data analytics and machine learning in patients with hepatocellular carcinoma after curative surgery: abridged secondary publication. Hong Kong Med J 2025;31(Suppl 1):S4-7.
2. Chan KW, Kwong ASK, Tsui PN, et al. Add-on astragalus therapy for diabetic kidney disease: an open-label randomised controlled trial with responder regression analysis (abridged secondary publication). Hong Kong Med J 2025;31(Suppl 1):S19-22.
3. Yeung NCY, Chan EYY, Cheng C, Mak WWS, Siu JYM, Cheung PSY. Tele-delivered supportive cancer care for breast cancer survivors: abridged secondary publication. Hong Kong Med J 2025;31(Suppl 1):S32-7.

Prediction of recurrence and survival using big data analytics and machine learning in patients with hepatocellular carcinoma after curative surgery: abridged secondary publication

EYP Lee *, M Kuo, KCK Ng, YC Wu, P Cao, CL Chiang, WCL Chan, TT Cheung, KWH Chiu

KEY MESSAGES

1. A deep-learning model was developed using preoperative computed tomography to predict hepatocellular carcinoma recurrence.
2. Compared with microvascular invasion, Recurr-NET demonstrated superior risk stratification in predicting hepatocellular carcinoma recurrence.
3. Recurr-NET can be used for preoperative prognostication in hepatocellular carcinoma.

Hong Kong Med J 2025;31(Suppl 1):S4-7
HMRF project number: 07182346

EYP Lee, M Kuo, KCK Ng, YC Wu, P Cao, CL Chiang, WCL Chan, TT Cheung, KWH Chiu

Department of Diagnostic Radiology, School of Clinical Medicine, LKS Faculty of Medicine, The University of Hong Kong, Hong Kong SAR, China

* Principal applicant and corresponding author: eyplee77@hku.hk

Introduction

Despite curative surgery, early recurrence of hepatocellular carcinoma (HCC) within 2 years remains common. Histological microvascular invasion (MVI) is strongly associated with early recurrence.[1] HCC is typically diagnosed via computed tomography (CT) or magnetic resonance imaging (MRI); the role of advanced imaging metrics for prediction of postoperative recurrence is important. Deep-learning techniques can automatically identify complex patterns and provide quantitative assessments of radiological findings. A CT-based deep-learning algorithm capable of predicting longitudinal, clinically relevant outcomes could substantially enhance HCC prognostication and management. We developed a deep-learning model using preoperative CT to predict HCC recurrence after curative surgery.

Methods

Consecutive patients diagnosed with resectable HCC at four medical centres in Hong Kong (internal cohort, December 2008 to December 2019) and one medical centre in Taiwan (external cohort, May 2006 to August 2019) were included. All patients were Chinese, aged ≥18 years, and underwent hepatic resection with histologically confirmed HCC. MVI was defined as tumour cells located in intra- or extra-tumoural blood vessels covered by endothelial cells, observable only via microscopy.[2] After curative surgery, all patients underwent contrast-enhanced CT of the liver with serum alpha-fetoprotein monitoring every 6 months. Recurrence was based on CT or MRI findings of LI-RADS (liver imaging reporting and data system) category 5 lesions or histological or mortality data recorded.

The internal cohort was randomly divided into training and internal validation groups at an 8:2 ratio. Deep learning was conducted using PyTorch 1.12.1. Processed triphasic CT scans and preoperative clinical data were used to develop Recurr-NET, which is a multimodal, multiphasic residual-network random survival forest deep-learning model designed to predict the risk of HCC recurrence within 5 years. Recurr-NET consists of two components: an image model based on the residual network (ResNet) structure and a random survival forest model. A 64-dimensional vector derived from the image model was combined with patients' clinical data in the random survival forest model to calculate a risk score. Three versions of the deep-learning model were trained: Recurr-NET^{CT}, Recurr-NET^{LITE}, and Recurr-NET. Recurr-NET^{CT} incorporated only CT images, whereas Recurr-NET^{LITE} incorporated CT images and basic clinical parameters (age, sex, hepatitis B surface antigen, hepatitis C virus antibody, history of fatty liver on imaging, alpha-fetoprotein levels, and the Model for End-stage Liver Disease score). Recurr-NET, the full model, incorporated both CT images and comprehensive clinical parameters including those listed above as well as smoking status, comorbidities, use of antiviral therapy for hepatitis B, and baseline blood test results. All three models were applied to the internal validation and external testing cohorts.

The diagnostic accuracy of Recurr-NET for predicting HCC recurrence was stratified by year and presented as the area under the receiver operating characteristic curve (AUROC), positive predictive value, and negative predictive value. Bootstrapping was performed to calculate 95% confidence intervals. The AUROC of Recurr-NET was compared with that of MVI using the Delong's test. Cumulative

TABLE 1. Characteristics of patients

Characteristic	All (n=1231)*	Training (n=536)*	Internal validation (n=135)*	External testing (n=560)*
Age, y	62.4±10.7	62.5±9.3	63.0±9.1	62.1±12.2
Male sex	1023 (83.1)	465 (86.8)	107 (79.3)	451 (80.5)
Ever-smoker	-	244 (45.5)	60 (44.4)	-
Liver disease				
Viral hepatitis	1068 (86.8)	478 (89.2)	120 (88.9)	470 (83.9)
Hepatitis B	943 (76.6)	445 (83.0)	109 (80.7)	389 (69.5)
Hepatitis C	144 (11.7)	35 (6.5)	11 (8.1)	98 (17.5)
Alcohol-related liver disease	-	35 (6.5)	9 (6.7)	-
Non-alcoholic fatty liver	-	6 (1.1)	1 (0.7)	-
Other liver diseases/cryptogenic	-	82 (15.3)	19 (14.1)	-
Barcelona Clinic Liver Cancer stage				
0	167 (13.6)	95 (17.7)	26 (19.3)	46 (8.2)
A	857 (69.6)	337 (62.9)	88 (65.2)	432 (77.1)
B	176 (14.3)	79 (14.7)	15 (11.1)	82 (14.6)
C	31 (2.5)	25 (4.7)	6 (4.4)	0
D	0	0	0	0
Blood tests				
Model for End-Stage Liver Disease score	8.0±2.2	8.2±2.2	8.0±2.0	7.9±2.3
Platelets, 10^9/L	176.6±78.0	173.5±75.1	177.1±86.4	179.3±78.7
Prothrombin time, s	11.6 (10.9-12.5)	12.2 (11.4-13.0)	12.2 (11.5-13.0)	11.1 (10.6-11.5)
Albumin, g/L	41.0 (38.0-44.0)	42.0 (38.0-44.0)	42.0 (38.0-44.0)	40.0 (38.0-43.0)
Alpha fetoprotein, ng/mL	15.7 (4.0-178.5)	15.0 (4.0-152.0)	10.0 (3.8-108.3)	18.4 (4.8-325.0)
Comorbidities				
Diabetes mellitus	303 (24.6)	155 (28.9)	32 (23.7)	116 (20.7)
Hypertension	511 (41.5)	231 (43.1)	59 (43.7)	221 (39.5)
Hyperlipidaemia	119 (9.7)	76 (14.2)	13 (9.6)	30 (5.4)
Chronic kidney disease	38 (3.1)	18 (3.4)	5 (3.7)	15 (2.7)
Ischaemic heart disease	56 (4.5)	25 (4.7)	7 (5.2)	24 (4.3)
Computed tomography findings				
No. of radiological lesions	1.6±1.0	2.0±1.2	2.0±1.2	1.2±0.5
Multiple lesions	441 (35.8)	281 (52.4)	68 (50.3)	92 (16.4)
Size of dominant lesion, cm	5.0±3.6	4.3±3.3	4.9±3.7	5.6±3.7
Major vessel involvement	52 (4.2)	18 (3.4)	3 (2.2)	31 (5.5)
Features of portal hypertension	264 (21.4)	141 (26.3)	35 (25.9)	88 (15.7)
Histological findings				
No. of hepatocellular carcinoma nodules	1.3±0.7	1.3±0.8	1.3±0.9	1.2±0.5
Multifocal hepatocellular carcinoma	206 (16.7)	102 (19.0)	19 (14.1)	85 (15.2)
Size of dominant lesion, cm	5.1±3.7	4.5±3.3	5.0±4.0	5.6±3.8
Microvascular invasion	591 (48.0)	159 (29.7)	35 (25.9)	397 (70.9)
Portal vein invasion	31 (2.5)	25 (4.7)	6 (4.4)	0
Margin involvement	85 (6.9)	38 (7.1)	5 (3.7)	42 (7.5)
Tumour differentiation				
Well differentiated	101 (8.2)	61 (11.4)	21 (15.6)	19 (3.4)
Moderately differentiated	716 (58.2)	334 (62.3)	79 (58.5)	303 (54.1)
Poorly differentiated	388 (31.5)	128 (23.9)	32 (23.7)	228 (40.7)
Undifferentiated	26 (2.1)	13 (2.4)	3 (2.2)	10 (1.8)
Cirrhosis in surrounding liver	501 (40.7)	270 (50.4)	61 (45.2)	170 (30.4)
Steatosis in surrounding liver	377 (30.6)	137 (25.6)	34 (25.2)	206 (36.8)

* Data are presented as mean ± standard deviation, median (range), or No. (%) of patients

recurrence risks predicted by Recurr-NET and MVI were plotted on Kaplan-Meier curves and compared in terms of survival difference at fixed time points.

Results

In total, 1231 patients with hepatic resection and histologically confirmed HCC were included in the analysis (Table 1). Among these, 536 (43.5%), 135 (11.0%), and 560 (45.5%) patients comprised the training, internal validation, and external testing cohorts, respectively. Overall, the median follow-up duration was 65.1 (range, 35.7-101.2) months. Cumulative probabilities of recurrence at 2 and 5 years were 41.8% and 56.4%, respectively. Overall, 568 (46.1%) patients died at a median interval of 35.0 (range, 17.0-64.7) months. In the internal cohort, 247 (36.8%) patients died of liver-related causes at a median interval of 32.6 (range, 16.3-61.8) months.

Recurr-NET achieved AUROCs of 0.770 to 0.857 in the internal validation cohort and 0.758 to 0.798 in the external testing cohort, significantly outperforming MVI in the respective cohorts (0.518 to 0.590 and 0.557 to 0.615) for predicting HCC recurrence from years 1 to 5 (all P<0.001, Table 2). The AUROCs for Recurr-NET^{LITE} and Recurr-NET^{CT} were also superior to those for MVI (all P<0.001) but remained numerically lower than those of the full Recurr-NET model.

Compared with MVI, Recurr-NET demonstrated superior risk stratification for recurrence at year 2 in the internal validation cohort (72.5% vs 50.0%, P<0.001) and external testing cohort (65.3% vs 46.6%, P<0.001) as well as for recurrence at year 5 in the respective cohorts (86.4% vs 62.5%, P<0.001 and 81.4% vs 63.8%, P<0.001) [Fig].

Patients identified as high-risk by Recurr-NET, compared with those identified by MVI, exhibited significantly higher liver-related mortality rates at year 2 (28.3% vs 11.8%, P<0.001) and year 5 (69.1% vs 29.9%, P<0.001). Similarly, Recurr-NET outperformed MVI in predicting all-cause mortality at year 2 in the internal validation cohort (31.9% vs 14.3%, P<0.001) and external testing cohort (32.7% vs 18.9%, P<0.001) as well as all-cause mortality at year 5 in the respective cohorts (72.9% vs 34.3, P<0.001 and 66.8% vs 37.9%, P<0.001).

Discussion

We developed, validated, and externally tested Recurr-NET, a multimodal multiphasic CT-based deep-learning model for predicting HCC recurrence and mortality after curative surgery. Recurr-NET demonstrated superior risk stratification compared with MVI, the principal histological predictor of aggressive tumour behaviour, for both early and late recurrence of HCC. Notably, the performance of Recurr-NET remained robust in external testing and across diverse patient subgroups stratified by age, viral hepatitis status, cirrhosis, and steatosis. A key advantage of Recurr-NET over MVI is its exclusive reliance on preoperative CT and clinical variables, facilitating prognostication before surgery.

By incorporating comprehensive preoperative imaging and clinical data, Recurr-NET demonstrated excellent performance in predicting both early and late recurrence, as well as liver-related and all-cause mortality. From a clinical perspective, Recurr-NET may assist in identifying patients at high risk of late recurrence, enabling clinicians to consider liver transplantation as an alternative to resection for these individuals.[3]

This study had some limitations. First, no centralised histological review was conducted; pathology findings were derived from reports generated by pathologists at each participating hospital. Second, because Recurr-NET was developed using CT data,

TABLE 2. Diagnostic accuracy of Recurr-NET^{CT}, Recurr-NET^{LITE}, Recurr-NET, and microvascular invasion for hepatocellular carcinoma recurrence

Model	Year 1					Year 2					Year 3					Year 4					Year 5				
	AUROC	PPV	NPV	SEN	SPE	AUROC	PPV	NPV	SEN	SPE	AUROC	PPV	NPV	SEN	SPE	AUROC	PPV	NPV	SEN	SPE	AUROC	PPV	NPV	SEN	SPE
Internal validation																									
Recurr-NET	0.843	0.659	0.868	0.692	0.849	0.857	0.744	0.807	0.653	0.866	0.838	0.857	0.739	0.610	0.915	0.809	0.884	0.607	0.535	0.911	0.770	0.884	0.543	0.507	0.898
Recurr-NET^{LITE}	0.811	0.769	0.821	0.513	0.935	0.762	0.828	0.755	0.490	0.939	0.760	0.893	0.667	0.424	0.958	0.742	0.906	0.558	0.408	0.946	0.757	0.939	0.516	0.413	0.959
Recurr-NET^{CT}	0.796	0.720	0.804	0.462	0.925	0.776	0.767	0.743	0.469	0.915	0.770	0.862	0.663	0.424	0.944	0.761	0.917	0.582	0.465	0.946	0.756	0.944	0.534	0.453	0.959
Microvascular invasion	0.590	0.441	0.755	0.385	0.796	0.570	0.500	0.670	0.347	0.793	0.547	0.545	0.577	0.305	0.789	0.541	0.636	0.468	0.296	0.786	0.518	0.636	0.407	0.280	0.755
External testing																									
Recurr-NET	0.798	0.488	0.882	0.729	0.726	0.781	0.668	0.789	0.699	0.764	0.759	0.749	0.683	0.637	0.785	0.758	0.817	0.604	0.613	0.812	0.760	0.863	0.513	0.556	0.841
Recurr-NET^{LITE}	0.760	0.570	0.844	0.563	0.848	0.740	0.708	0.718	0.505	0.858	0.711	0.788	0.610	0.439	0.881	0.740	0.861	0.556	0.479	0.894	0.752	0.890	0.486	0.474	0.894
Recurr-NET^{CT}	0.755	0.600	0.852	0.583	0.860	0.706	0.686	0.709	0.486	0.849	0.693	0.786	0.608	0.435	0.881	0.720	0.858	0.559	0.489	0.889	0.734	0.915	0.500	0.490	0.918
Microvascular invasion	0.615	0.327	0.888	0.875	0.354	0.605	0.476	0.769	0.833	0.377	0.590	0.565	0.654	0.798	0.383	0.568	0.623	0.546	0.792	0.343	0.557	0.678	0.459	0.784	0.329

Abbreviations: AUROC=area under receiver operating characteristic curve, NPV=negative predictive value, PPV=positive predictive value, SEN=sensitivity, SPE=specificity

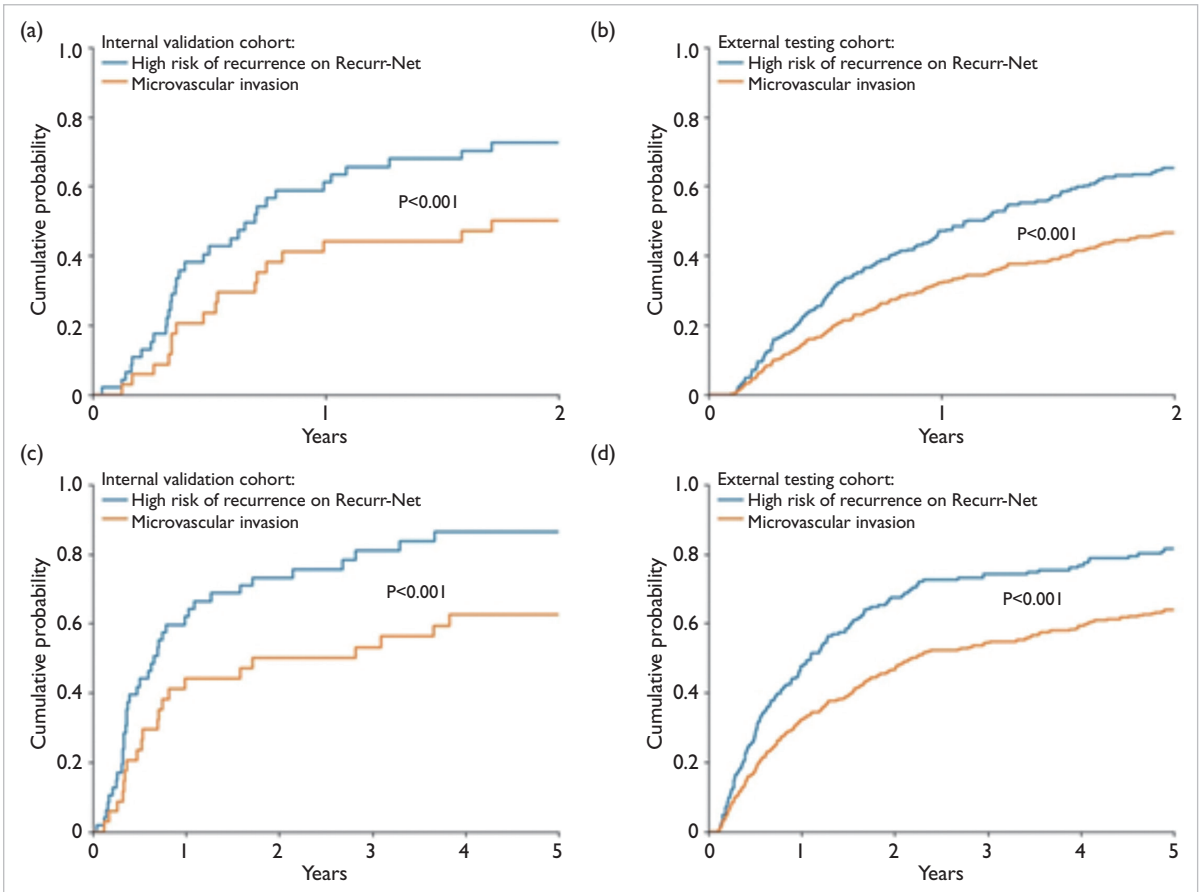

FIG. Comparison of Recurr-NET with microvascular invasion for recurrence risk stratification. Cumulative probabilities of hepatocellular carcinoma recurrence for internal validation and external testing cohorts at (a and b) year 2 and (c and d) year 5 are shown

its findings cannot be directly extrapolated to MRI-based assessments. However, the random survival forest component of Recurr-NET allowed integration of a Kaplan-Meier estimator for survival analysis. This enabled consideration of time as a factor, facilitating the determination of clinically relevant outcomes such as HCC recurrence and mortality. Additionally, we specifically collected longitudinal data over a period of 5 years (median, 65.1 months) to evaluate both early and late HCC recurrence. The use of external testing validated the promising diagnostic and risk stratification performance of Recurr-NET, suggesting that our findings are robust and generalisable.

Conclusions

Recurr-NET, which utilises preoperative CT and clinical parameters, demonstrated robust risk stratification for early and late HCC recurrence and mortality after curative surgery. The model consistently outperformed MVI in recurrence risk stratification, demonstrating its potential use for preoperative prognostication.

Funding

This study was supported by the Health and Medical Research Fund, Health Bureau, Hong Kong SAR Government (#07182346). The full report is available from the Health and Medical Research Fund website (https://rfs2.healthbureau.gov.hk).

Disclosure

The results of this research have been previously published in:

1. Hui RW, Chiu KW, Lee IC, et al. Multimodal multiphasic pre-operative image-based deep-learning predicts hepatocellular carcinoma outcomes after curative surgery. Hepatology 2024 Dec 2.

References

1. Erstad DJ, Tanabe KK. Prognostic and therapeutic implications of microvascular invasion in hepatocellular carcinoma. Ann Surg Oncol 2019;26:1474-93.
2. Nitta H, Allard MA, Sebagh M, et al. Prognostic value and prediction of extratumoral microvascular invasion for hepatocellular carcinoma. Ann Surg Oncol 2019;26:2568-76.
3. Hui RW, Mak LY, Cheung TT, Lee VH, Seto WK, Yuen MF. Clinical practice guidelines and real-life practice on hepatocellular carcinoma: the Hong Kong perspective. Clin Mol Hepatol 2023;29:217-29.

Artificial intelligence for prostate cancer detection and classification on magnetic resonance imaging: abridged secondary publication

P Cao *, V Vardhanabhuti, W Lam

KEY MESSAGES

1. We used CapsuleNet for prostate lesion detection and classification via the Prostate Imaging Reporting and Data System, incorporating relative spatial information and the clinical context of lesions in relation to various anatomical structures.
2. Deep learning methods for CapsuleNet classification have only achieved satisfactory outcomes. To improve outcomes, we used MiniSegCaps, an end-to-end network that integrates classification and segmentation, specifically designed for a small dataset.
3. MiniSegCaps demonstrated impressive performance. We also developed a graphical user interface to illustrate its integration with the clinical workflow.

Hong Kong Med J 2025;31(Suppl 1):S8-10
HMRF project number: 07182706

[1] **P Cao**, [1] **V Vardhanabhuti**, [2] **W Lam**

[1] *Department of Diagnostic Radiology, The University of Hong Kong, Hong Kong SAR, China*
[2] *Department of Urology, The University of Hong Kong, Hong Kong SAR, China*

* Principal applicant and corresponding author: caopeng1@hku.hk

Introduction

Magnetic resonance imaging (MRI) is the primary imaging modality for diagnosing prostate cancer. The Prostate Imaging Reporting and Data System (PI-RADS) for multiparametric MRI provides essential MRI interpretation guidelines but is subject to inter-reader variability.[1,2] MRI-guided biopsy is increasingly favoured for risk assessment, replacing the conventional transrectal ultrasound-guided biopsy.[3] The growing demand for prostate MRI has led to an increase in referrals, increasing radiologists' workload.[4] The PI-RADS facilitates the classification of lesions based on risk and demonstrates high sensitivity in the detection of high-grade prostate lesions.[5] However, it displays poor inter-reader and intra-reader consistency; thus, substantial expertise is necessary. Less experienced radiologists exhibit greater inter-reader variability in PI-RADS scoring.

Deep learning networks facilitate automatic lesion segmentation and classification, reducing radiologists' workload and mitigating inter-reader variability. Deep learning–based lesion detection and PI-RADS classification algorithms are essential for integrating prostate MRI findings into clinical practice. Some networks can differentiate prostate cancer from normal tissues and calculate the probability of malignancy. Current methods for PI-RADS classification remain semi-automated; lesion masks must be manually entered into the model. These convolutional neural networks require substantial annotated data and data augmentation to address class imbalance. Few networks integrate lesion detection and classification tasks within a single framework and achieve reliable performance at a PI-RADS cutoff value of ≥4.

In PI-RADS, classification depends not only on lesion dimensions, edge morphology, and signal intensity but also on positional relationships (such as extraprostatic extension/invasion) and zonal location relative to the transition and peripheral zones.[5] Each lesion is assigned a score of 1 to 5 based on diffusion-weighted and T2-weighted MRI, along with the presence or absence of dynamic contrast enhancement. The contribution of these scores to the overall PI-RADS assessment varies depending on the lesion's zonal location. For lesions in the transition zone, the PI-RADS score is primarily determined by the T2-weighted score, and the diffusion-weighted imaging score serves as a modifier. For lesions in the peripheral zone, the diffusion-weighted imaging score is predominant, and the presence of dynamic contrast enhancement serves as a modifier.[5] These spatial relationships and lesion features (location, scale, and dimension) can be encoded and represented by CapsNet in a single capsule vector, enabling prostate cancer detection and classification. We aimed to compare our MiniSegCaps model with baseline segmentation methods for prostate cancer segmentation and classification.

Methods

Of 569 patients who underwent multiparametric

MRI (including T2-weighted, diffusion-weighted, and dynamic contrast-enhanced sequences) at our institution, 494 had one or more detectable prostate cancer lesions classified by radiologists based on their PI-RADS score.[5] Of these patients, 32 were excluded owing to a history of prostate cancer treatment (including antihormonal therapy, radiation therapy, focal therapy, and prostatectomy) or the presence of an incomplete MRI sequence. Thus, 462 patients with a PI-RADS score of ≥1 were included in the analysis.

We used a multitask network—MiniSegCaps—which is an end-to-end multiclass VNet designed to jointly segment prostate lesions and predict their PI-RADS categories. Selected for its robust performance on small datasets, MiniSegCaps is based on MiniSeg and follows a U-Net-like encoder-decoder architecture.

The encoder and decoder of MiniSeg extract high-dimensional features from input images and generate segmentation outputs, respectively. The model uses three-channel input comprising T2-weighted images, apparent diffusion coefficient maps, and zonal masks (Figs 1 and 2). The encoder processes image data into high-dimensional features through a series of convolutional blocks, which are further processed by capsules in subsequent layers. The capsule predictive branch includes two convolutional capsule layers that encode spatial information about objects into capsule vectors. The number of capsule types in the final convolutional capsule layer corresponds to the number of segmentation categories, which are supervised by a margin loss. This branch is specifically designed to predict binary high-grade or low-grade PI-RADS categories.

To support radiologists in the clinical diagnosis of prostate cancer, we developed a graphical user interface integrated into the overall workflow to automatically generate prostate cancer diagnostic reports. These reports include the predicted lesion mask, lesion visualisation on T2-weighted images and apparent diffusion coefficient maps, predicted probabilities for each PI-RADS category, and the position and dimensions of each lesion. The main steps of the workflow within the graphical user interface include image data importation, zonal segmentation, lesion overlay on multiparametric MRI, image preprocessing (cropping and normalisation), lesion segmentation, PI-RADS classification, and diagnostic report generation.

Results

We compared our MiniSegCaps model with baseline segmentation methods for prostate cancer segmentation using the Dice coefficient metric. Additionally, we implemented a combined version of MiniSeg and CapsuleNet, supervised with ordinal encoding ground truths, to demonstrate the effectiveness of incorporating capsule layers into MiniSegCaps.

Among baseline methods, two-dimensional U-Net, attention U-Net, and U-Net++ achieved an average Dice coefficient of 51%, which was lower than the 65% achieved by MiniSeg in image-level evaluations. Performance in patient-level evaluations followed a similar trend, indicating that the lightweight MiniSeg model performs better when handling small datasets.

Both MiniSegCaps and MiniSegCaps without CapsGRU substantially outperformed MiniSeg, SegNet, and FocalNet. This result indicates that the integration of capsule layers into MiniSegCaps enables better differentiation of prostate cancer from normal tissues by capturing the relative spatial relationships between prostate cancer and various anatomical structures.

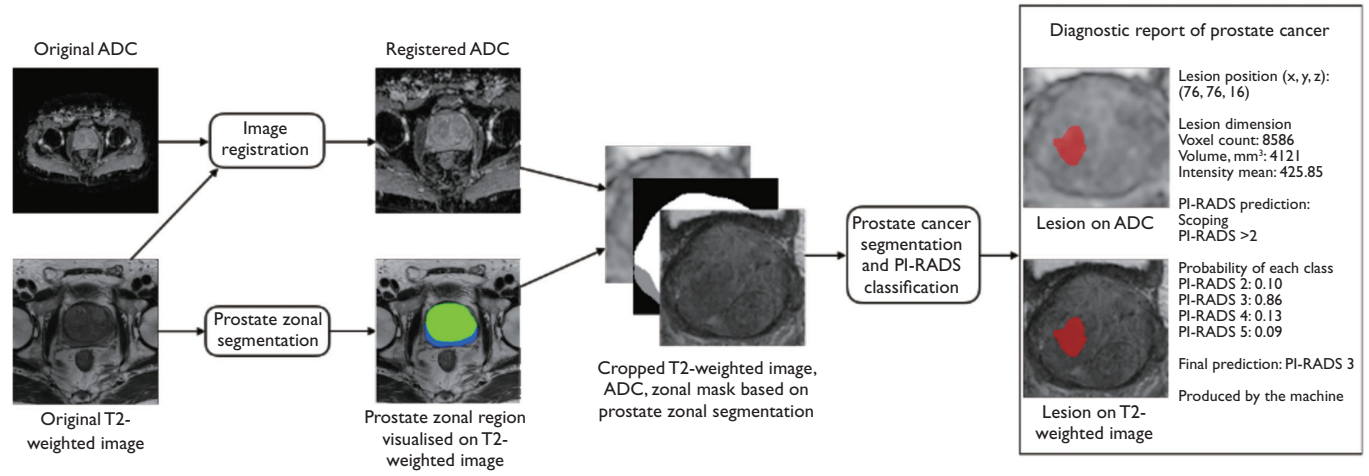

FIG 1. Step 1: image preprocessing (registration and normalisation); step 2: zonal segmentation and cropping; step 3: prostate cancer segmentation and classification; and step 4: diagnostic report generation

Abbreviations: ADC=apparent diffusion coefficient, PI-RADS=Prostate Imaging Reporting and Data System

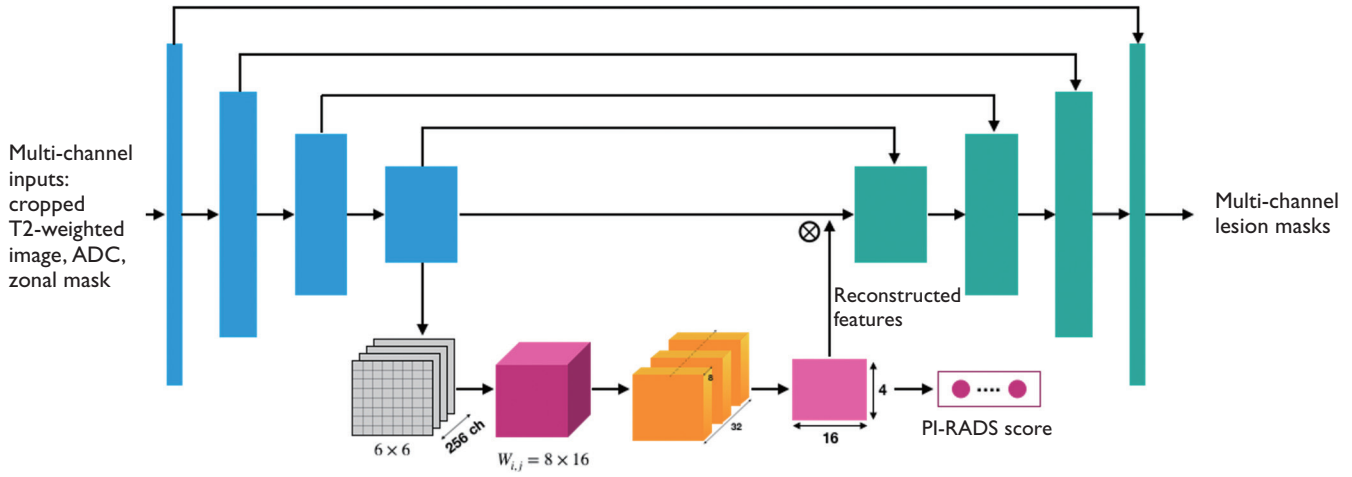

FIG 2. The architecture of the proposed MiniSegCaps model includes MiniSeg (a lightweight segmentation network serving as the backbone for lesion mask prediction), a capsule predictive branch for PI-RADS scoring, and a CapsGRU module for utilising spatial information across adjacent slices. The MiniSeg module extracts convolutional feature maps from input multiparametric MRI and generates multi-channel masks for prostate cancer segmentation. Features learned by the final downsampling block of MiniSeg (6×6×256) are used as inputs for the capsule predictive branch to perform PI-RADS classification. Capsule feature stacks (8×32) generated by PrimaryCaps are processed by the CapsGRU module to incorporate inter-slice spatial information during the learning process. Reconstructed features (6×6×256) produced by three fully connected layers in the capsule branch are also integrated into the MiniSeg module to enhance lesion identification

Abbreviations: ADC=apparent diffusion coefficient, MRI=magnetic resonance imaging, PI-RADS=Prostate Imaging Reporting and Data System

For PI-RADS classification, the average accuracies of three categories produced by baseline methods were 57% (PI-RADS ≥3), 63% (PI-RADS ≥4), and 65% (PI-RADS ≥5) in patient-level evaluation, slightly exceeding the corresponding results in image-level evaluation. MiniSegCaps (comprising a convolutional encoder, a deconvolutional decoder with fused feature inputs, and a Capsule predictive branch with CapsGRU) outperformed MiniSegCaps without CapsGRU and the combined MiniSeg and CapsuleNet model. The inclusion of CapsGRU in MiniSegCaps improved consistency across adjacent slices, enhancing PI-RADS classification performance. Consequently, MiniSegCaps achieved the highest accuracy in all PI-RADS categories. It also increased the accuracy of PI-RADS classification by an average of 15% in patient-level evaluation, compared with MiniSeg (or VNet).

For binary high-grade/low-grade PI-RADS classification, MiniSegCaps achieved a patient-level accuracy of 71.56% and a sensitivity of 76.32% for high-grade lesions (PI-RADS ≥4). CapsGRU further enhanced the overall performance of binary high-grade/low-grade lesion differentiation, compared with MiniSegCaps without CapsGRU.

Conclusion

Our MiniSegCaps model jointly predicted lesion segmentation and PI-RADS classification, achieving superior performance in prostate cancer segmentation and PI-RADS classification compared with other methods. Its performance for PI-RADS ≥3, a critical threshold in clinical decision-making, was particularly robust.

Funding

This study was supported by the Health and Medical Research Fund, Health Bureau, Hong Kong SAR Government (#07182706). The full report is available from the Health and Medical Research Fund website (https://rfs2.healthbureau.gov.hk).

Disclosure

The results of this research have been previously published in:

1. Jiang W, Lin Y, Vardhanabhuti V, Ming Y, Cao P. Joint Cancer Segmentation and PI-RADS Classification on Multiparametric MRI Using MiniSegCaps Network. Diagnostics (Basel) 2023;13:615.

References

1. International Agency for Research on Cancer. Global Cancer Observatory: Cancer Today. Available from: https://gco.iarc.fr/today/home/
2. Ahmed HU, El-Shater Bosaily A, Brown LC, et al. Diagnostic accuracy of multi-parametric MRI and TRUS biopsy in prostate cancer (PROMIS): a paired validating confirmatory study. Lancet 2017;389:815-22.
3. Kasivisvanathan V, Rannikko AS, Borghi M, et al. MRI-targeted or standard biopsy for prostate-cancer diagnosis. N Engl J Med 2018;378:1767-77.
4. Leake JL, Hardman R, Ojili V, et al. Prostate MRI: access to and current practice of prostate MRI in the United States. J Am Coll Radiol 2014;11:156-60.
5. Barrett T, Turkbey B, Choyke PL. PI-RADS version 2: what you need to know. Clin Radiol 2015;70:1165-76.

Light-based depth-sensing device with deep learning to measure spinal deformity: abridged secondary publication

T Zhang *, JPY Cheung, KKY Wong

KEY MESSAGES

1. A light-based depth-sensing device with deep learning offers a rapid, non-invasive method for spine examination and has potential for integration into routine scoliosis screening for adolescents.
2. The device demonstrates promising performance in scoliosis assessment.
3. This screening tool may be beneficial in resource-constrained or remote regions such as those with a shortage of radiographic medical imaging devices or specialists.

Hong Kong Med J 2025;31(Suppl 1):S11-3
HMRF project number: 08192266

[1] T Zhang, [1] JPY Cheung, [2] KKY Wong

[1] *Department of Orthopaedics and Traumatology, The University of Hong Kong, Hong Kong SAR, China*
[2] *Department of Computer Science, The University of Hong Kong, Hong Kong SAR, China*

* Principal applicant and corresponding author: tgzhang@hku.hk

Introduction

Scoliosis is a three-dimensional spinal deformity, defined by a Cobb angle (ie, angle formed by the upper endplate of the uppermost tilted vertebra and lower endplate of the lowermost tilted vertebra in the structural curve) of >10° on standing plain radiographs.[1] Among scoliosis types (idiopathic, congenital, neuromuscular, and syndromic), adolescent idiopathic scoliosis (AIS) is most common in the paediatric population. In Hong Kong, the prevalences of AIS are 2.2% in boys and 4.8% in girls.[2,3] Untreated cases can rapidly progress during the pubertal growth spurt, causing body disfigurement, cardiopulmonary compromise, and back pain.[4,5] Additionally, spinal degeneration may damage surrounding muscles, ligaments, and joint structures, thereby exacerbating pain and causing additional physical limitations. Early detection and intervention to prevent curve progression are therefore essential. Clinical screening and diagnosis currently require physical and radiographic examinations, which are subjective or associated with radiation exposure. We developed and validated a radiation-free portable device that uses light-based depth-sensing and deep-learning technologies to analyse AIS via landmark detection and image synthesis.

Methods

Consecutive patients with AIS who were treated in two scoliosis clinics in Hong Kong between 1 November 2021 and 31 March 2023 were recruited. Patients were excluded if they had psychological and/or systematic neural disorders that could affect compliance and/or mobility. For each participant, a red-green-blue depth image of the nude back was captured using our light-based depth-sensing device (Fig). Manually labelled landmarks and alignment parameters identified by our spine surgeons were considered the ground truth. Images from training and internal validation cohorts (n=1936) were used to develop the deep learning models. The model was then prospectively validated on another cohort (n=302) from Hong Kong with similar demographics. We evaluated the model's accuracy in detecting anatomical landmarks on the nude back and its performance in synthesising radiograph-comparable images (RCIs). These RCIs contain sufficient anatomical information to quantify disease severity and identify curve type.

Results

Our model consistently demonstrated high accuracy in predicting anatomical landmarks on the nude back, with a mean Euclidian and Manhattan distance error of <4 pixels. Using radiographic assessments by spine specialists as the ground truth, the synthesised RCIs achieved a sensitivity of >0.909 and a negative predictive value of >0.933 for AIS severity classification; the corresponding values for curve type classification were 0.974 and 0.908. Estimated Cobb angles from the synthesised RCIs were strongly correlated with ground truth angles (R^2=0.984, P<0.001).

Discussion

The light-based depth-sensing device with deep learning offers a rapid, non-invasive method for

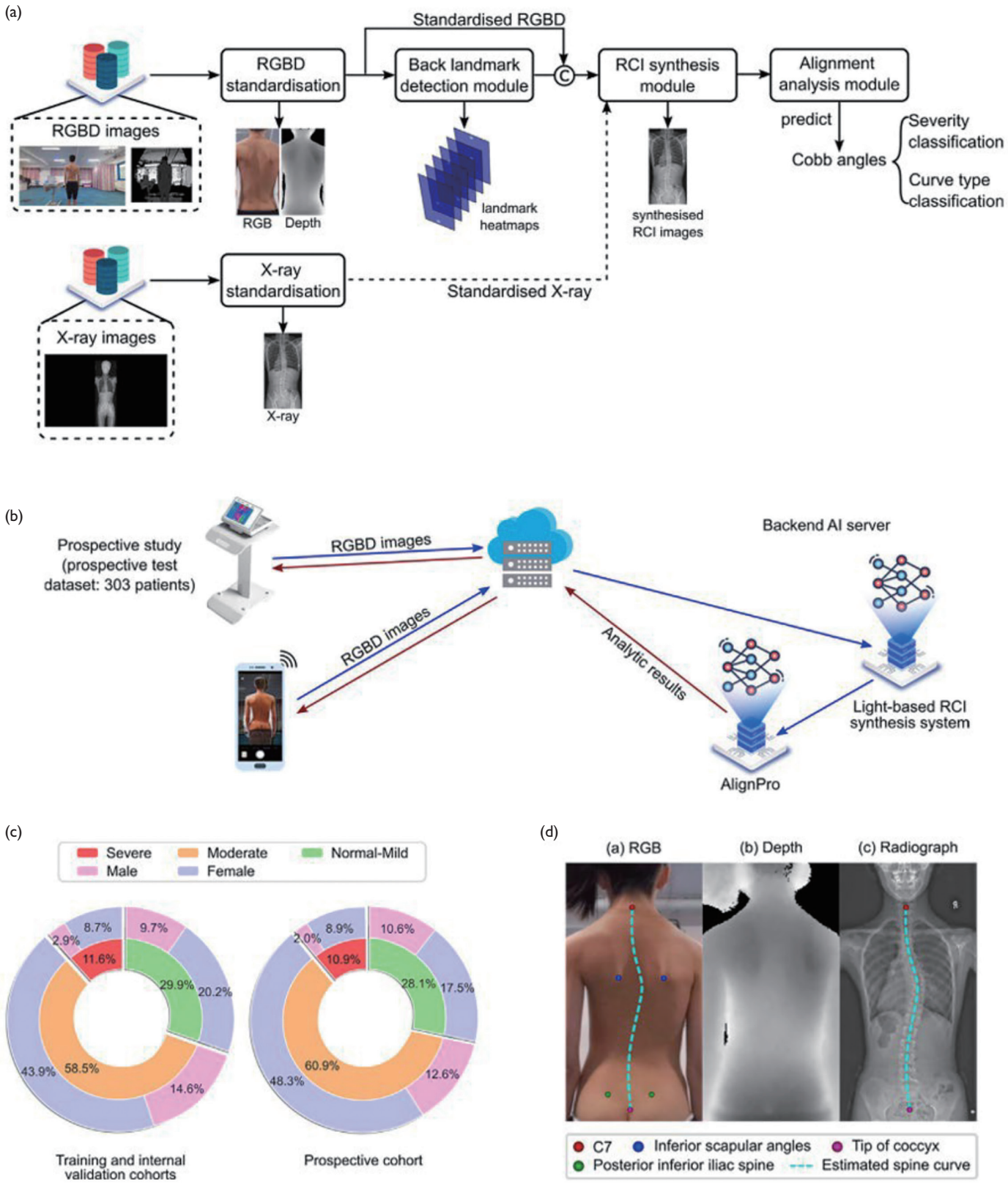

FIG. (a) The workflow of the light-based radiograph-comparable image (RCI) synthesis system, which comprises a red-green-blue depth (RGBD) and radiograph standardisation module, a back landmark detection module, a landmark-guided RCI synthesis module, and a quantitative alignment analysis module. The first module uses rule-based and adaptive algorithms to standardise images, whereas the other three modules use deep learning techniques. (b) RGBD images captured with a smartphone and our equipment are transmitted to a cloud data centre for analysis by the backend artificial intelligence server that hosts the light-based RCI synthesis and AlignPro system. Results are then transmitted back to the smartphone and equipment for display. (c) Pie charts showing proportions of different severity levels and sexes in all participants. (d) Examples of an RGB image, a depth image, and a corresponding radiograph

spine examination and has potential for integration into routine scoliosis screening for adolescents. The device demonstrates promising performance in scoliosis assessment. This screening tool may be beneficial in resource-constrained or remote regions such as those with a shortage of radiographic medical imaging devices or specialists. International multicentre trials are needed to assess the effects of demographic variables such as body mass index and skin colour, and to enhance device reliability before clinical use.

Funding

This study was supported by the Health and Medical Research Fund, Health Bureau, Hong Kong SAR Government (#08192266). The full report is available from the Health and Medical Research Fund website (https://rfs2.healthbureau.gov.hk).

Disclosure

The results of this research have been previously published in:

1. Meng N, Wong KYK, Zhao M, Cheung JP, Zhang T. Radiograph-comparable image synthesis for spine alignment analysis using deep learning with prospective clinical validation. eClinicalMedicine 2023;61:102050.

References

1. Cobb J. Outlines for the study of scoliosis. J Bone Joint Surg 1948.
2. Fong DY, Cheung KM, Wong YW, et al. A population-based cohort study of 394,401 children followed for 10 years exhibits sustained effectiveness of scoliosis screening. Spine J 2015;15:825-33.
3. Luk KD, Lee CF, Cheung KM, et al. Clinical effectiveness of school screening for adolescent idiopathic scoliosis: a large population-based retrospective cohort study. Spine (Phila Pa 1976) 2010;35:1607-14.
4. Yang J, Zhang K, Fan H, et al. Development and validation of deep learning algorithms for scoliosis screening using back images. Commun Biol 2019;2:390.
5. Weinstein SL, Dolan LA, Spratt KF, Peterson KK, Spoonamore MJ, Ponseti IV. Health and function of patients with untreated idiopathic scoliosis: a 50-year natural history study. JAMA 2003;289:559-67.

Data-driven analysis of carrier frequencies of autosomal recessive and X-linked diseases in the Asian population: abridged secondary publication

S Gu *, FM Lo, KWS Tsui, N Mullapudi

KEY MESSAGES

1. A robust pipeline was established to estimate and rank carrier frequencies of all known recessive genes based on genome-wide sequencing data in healthy individuals, with a focus on Asian populations.
2. Comprehensive criteria were applied to identify multiple deleterious variants including known pathogenic variants, presumed loss-of-function variants, predicted deleterious missense variants, and potentially harmful in-frame insertion and deletion mutations.
3. A high degree of correlation among different Asian population cohorts confirmed the validity of the variant selection criteria and overall analysis pipeline.

Hong Kong Med J 2025;31(Suppl 1):S14-8
HMRF project number: 08191216

[1] **S Gu**, [2] **FM Lo**, [1] **KWS Tsui**, [3] **N Mullapudi**

[1] *School of Biomedical Sciences, The Chinese University of Hong Kong, Hong Kong SAR, China*
[2] *Clinical Genetic Service, Department of Health, Hong Kong SAR, China*
[3] *Bionano Genomics, California, United States*

* Principal applicant and corresponding author: shengu@cuhk.edu.hk

Introduction

Single-gene disorders are common causes of neonatal and paediatric morbidity and mortality. Parents of individuals with autosomal recessive diseases and mothers of individuals with X-linked recessive diseases are carriers. Expanded newborn screening (NBS) and prenatal or pre-pregnancy expanded carrier screening (ECS) for recessive diseases are widely implemented in developed countries. Because carrier frequencies of recessive diseases vary among ethnic groups, recessive gene panels for NBS and ECS should be based on population-specific carrier frequencies in countries and regions with a single majority ethnic group.

Carrier frequencies for relatively large gene panels (eg, >100 genes) are primarily estimated using genome-wide sequencing data from unaffected individuals.[1-3] However, studies of carrier frequencies for large gene panels among individuals receiving genetic testing have been limited.[4,5] Both estimated and actual population-specific carrier frequencies are mostly based on individuals residing in the United States with self-reported ethnicities. In regions without accessible ECS, carrier frequencies for most genes remain unknown. This study aimed to develop an unbiased and robust pipeline for ranking carrier frequencies of all known recessive genes using genome-wide sequencing data. It also aimed to establish selection criteria for deleterious variants.

Methods

A combined list of type 1 to 4 variants (known pathogenic variants, presumed loss-of-function variants, predicted deleterious missense variants, and potentially harmful in-frame insertion and deletion mutations, respectively) was generated for each of the 2699 genes (Fig 1). Ethnicity-specific allele counts and total allele numbers were analysed for each variant, along with the number of individuals homozygous for each variant. The ethnicity-specific variant carrier rate (VCR) was also calculated. Each of the 2699 lists comprised the ethnicity-specific VCRs for each variant. The ethnicity-specific gene carrier rate (GCR) for each of the 2699 genes was then calculated, along with predicted genetic prevalence at the gene level (pGPg).

Spearman rank correlation coefficients and Pearson correlation coefficients were calculated. For correlation analysis between two datasets, only genes with a GCR >0 in at least one dataset were included. Statistical analyses were performed using R 3.6.0 and ggpubr 0.4.0.

Results

Selection of deleterious variants in recessive genes

Sequencing results from the publicly available Genome Aggregation Database (gnomAD) were extracted as the discovery cohort. In total, 2699 known disease-causing recessive genes were considered, including 2525 autosomal recessive genes and 174 X-linked genes. High-quality gnomAD variants aligned to the GRCh38 human genome assembly reference for each gene were processed.

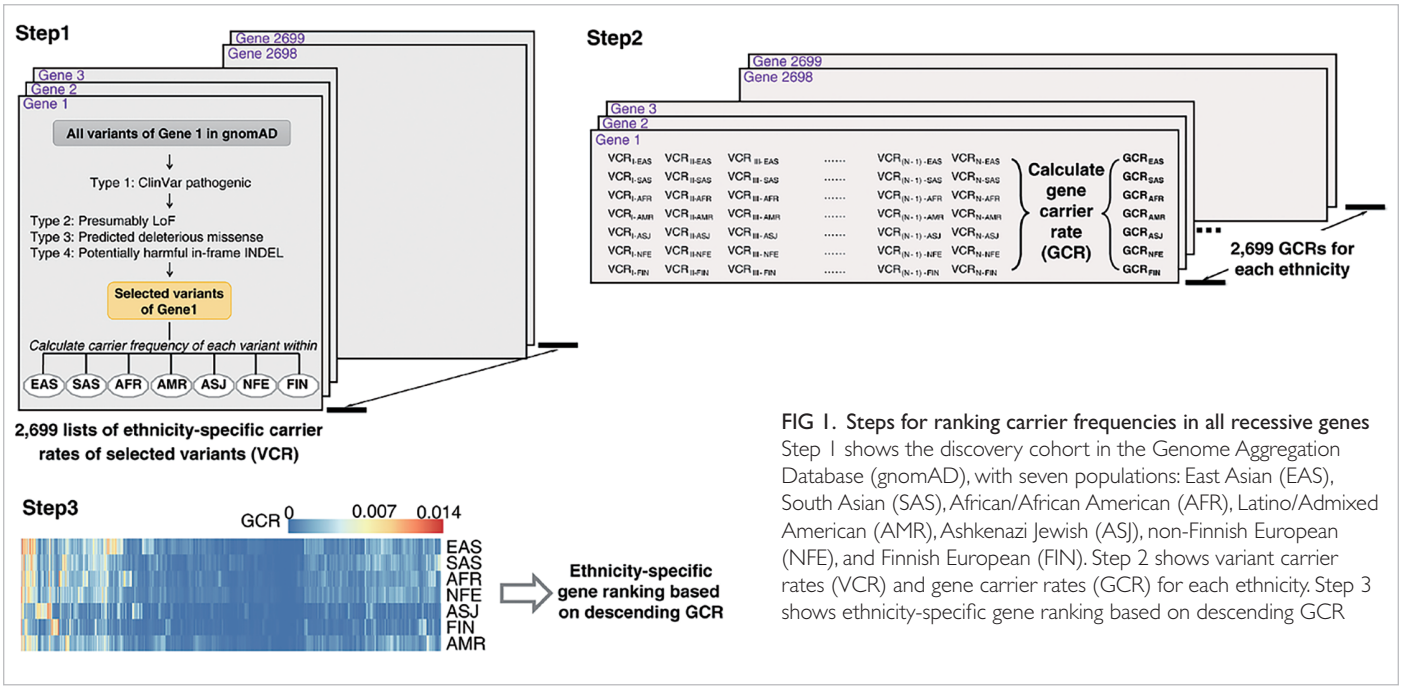

FIG 1. Steps for ranking carrier frequencies in all recessive genes
Step 1 shows the discovery cohort in the Genome Aggregation Database (gnomAD), with seven populations: East Asian (EAS), South Asian (SAS), African/African American (AFR), Latino/Admixed American (AMR), Ashkenazi Jewish (ASJ), non-Finnish European (NFE), and Finnish European (FIN). Step 2 shows variant carrier rates (VCR) and gene carrier rates (GCR) for each ethnicity. Step 3 shows ethnicity-specific gene ranking based on descending GCR

Overall, 48 198 273 gnomAD variants were identified in the 2699 genes. Among these variants, we selected those that were either reported in affected patients or potentially able to induce deleterious effects on gene function. Four types of variants were retained: known pathogenic variants (type 1), presumed loss-of-function variants (type 2), predicted deleterious missense variants (type 3), and potentially harmful in-frame insertion and deletion mutations (type 4).

Ethnicity-specific ranking of carrier frequencies in the discovery cohort

Seven sets of VCRs were identified for each ethnicity in each gene, resulting in seven sets of ethnicity-specific GCRs. Genes were then ranked by descending GCR values for each ethnicity. Consequently, genes with the highest GCRs (highest probabilities of causing recessive diseases in offspring) appeared at the top of the list for each population (Fig 1).

Ranking of carrier frequencies in validation cohorts

To verify the pipeline for ranking carrier frequencies, we analysed variants in three independent genome databases using whole-genome sequencing data from East Asian (Chinese) and South Asian (Malay and Indian) populations. These databases included the Singapore 10K Genome Project, China Metabolic Analytics Project (ChinaMAP), and Westlake BioBank for Chinese (WBBC) pilot project (Fig 2). Comparisons of results from different cohorts with similar ethnic backgrounds showed a high degree of correlation, confirming the validity of the variant selection criteria and overall analysis pipeline (Fig 3).

Carrier frequencies for genes in Hong Kong's newborn screening

In Hong Kong's NBS programme, among the 44 genes associated with 24 types of inborn errors of metabolism, six showed positive cases in the local population; their GCRs were generally high as expected. For some genes without positive cases, their GCRs were particularly low. This suggests a need to reconsider the selection of diseases and genes for a customised panel for the local population.

Discussion

We established a robust pipeline to estimate and rank carrier frequencies for all known recessive genes using genome-wide sequencing data. We developed comprehensive selection criteria for four types of potentially disease-causing variants and then confirmed the reliability of our filtering criteria.

Carrier frequencies of recessive diseases vary markedly among populations. The widespread use of next-generation sequencing has enabled the acquisition of carrier frequencies for large number of genes through both estimates based on large-scale genome-wide sequencing data and observations from ECS results. The former approach primarily focuses on individual genes or specific disease spectrums, whereas the latter approach focuses on genes included in the ECS panel. We performed

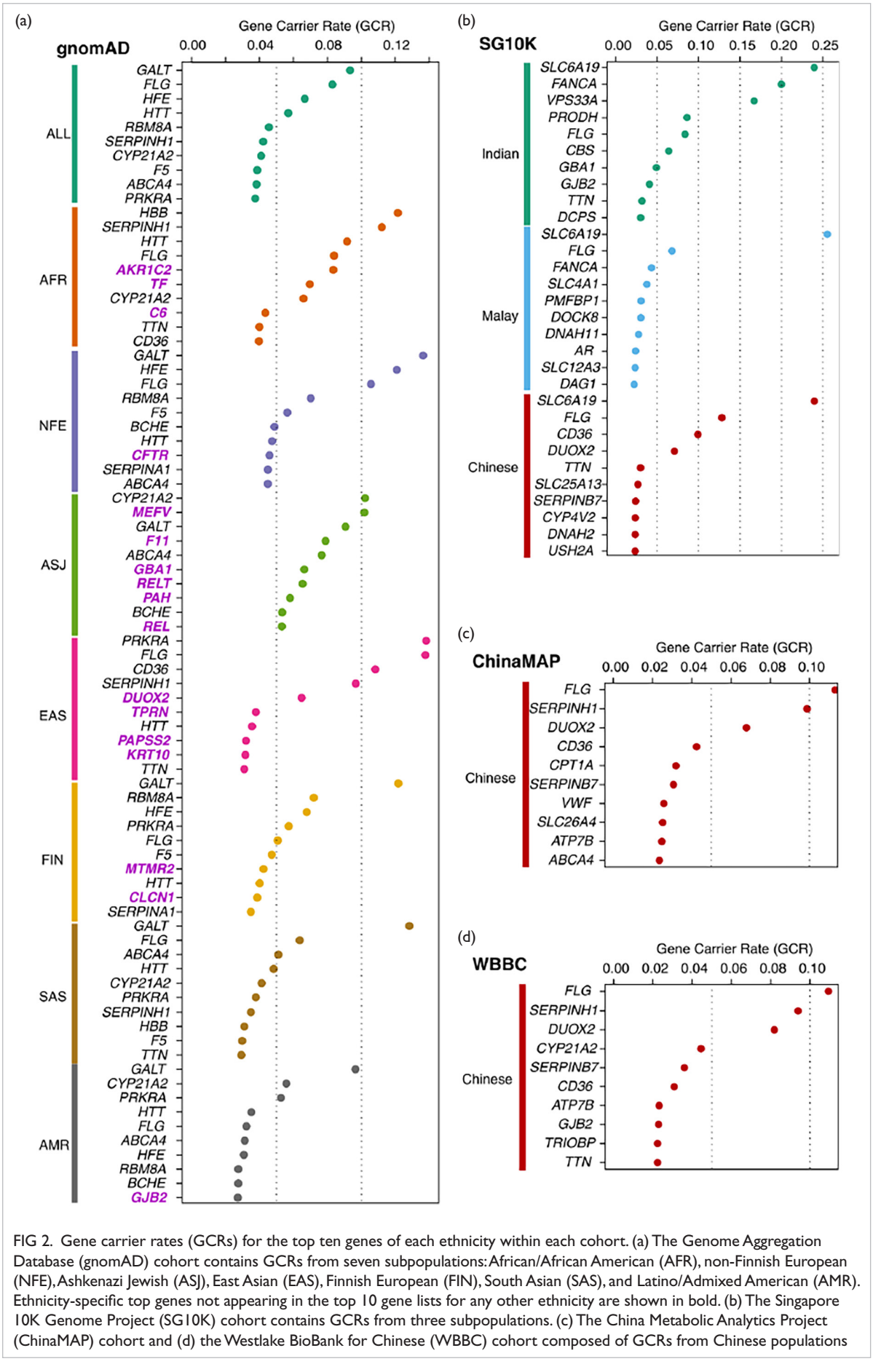

FIG 2. Gene carrier rates (GCRs) for the top ten genes of each ethnicity within each cohort. (a) The Genome Aggregation Database (gnomAD) cohort contains GCRs from seven subpopulations: African/African American (AFR), non-Finnish European (NFE), Ashkenazi Jewish (ASJ), East Asian (EAS), Finnish European (FIN), South Asian (SAS), and Latino/Admixed American (AMR). Ethnicity-specific top genes not appearing in the top 10 gene lists for any other ethnicity are shown in bold. (b) The Singapore 10K Genome Project (SG10K) cohort contains GCRs from three subpopulations. (c) The China Metabolic Analytics Project (ChinaMAP) cohort and (d) the Westlake BioBank for Chinese (WBBC) cohort composed of GCRs from Chinese populations

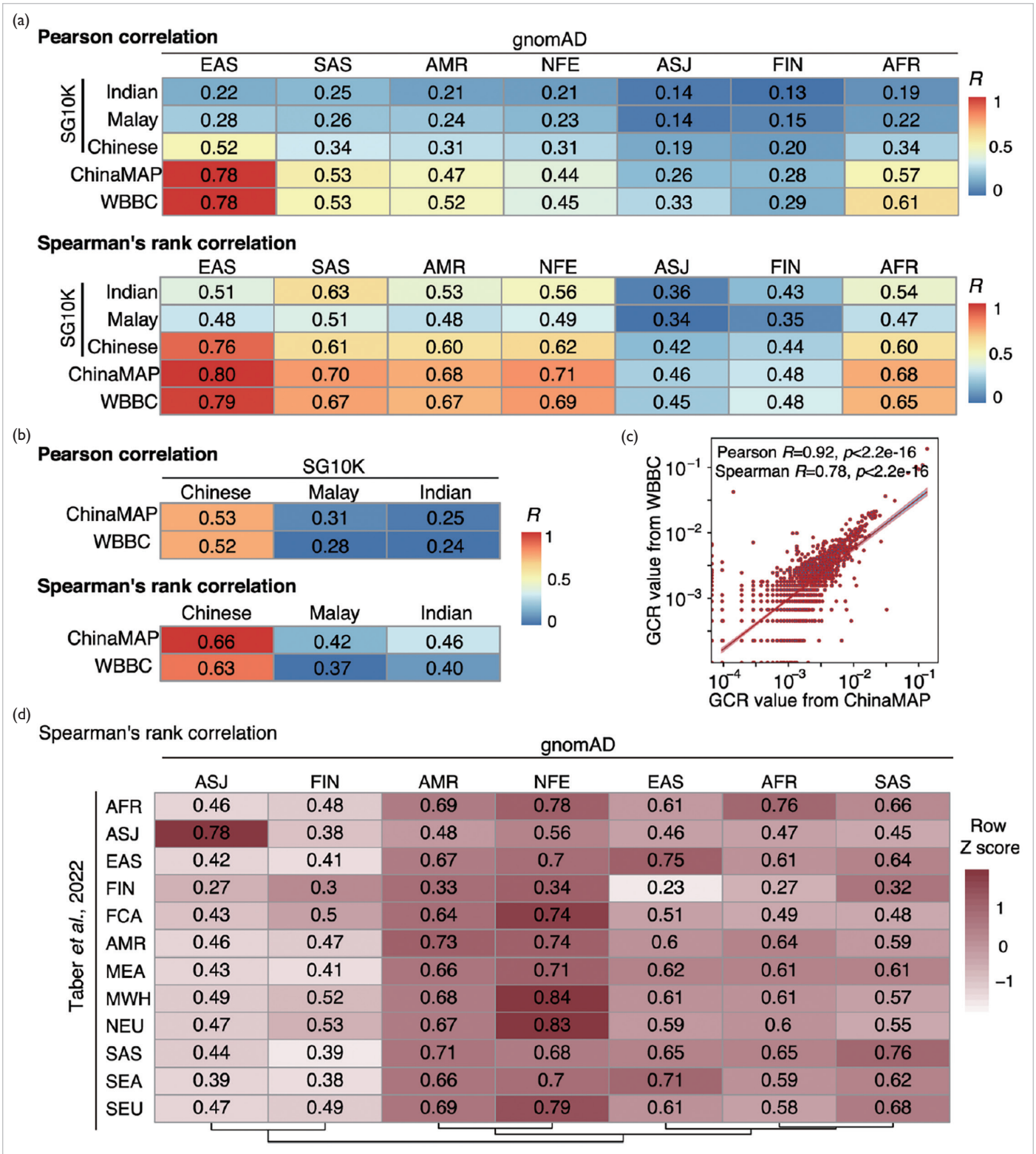

FIG 3. Comparison of carrier frequencies among cohorts. (a) Comparison between Genome Aggregation Database (gnomAD) populations and Singapore 10K Genome Project (SG10K) subpopulations, China Metabolic Analytics Project (ChinaMAP) Chinese, or Westlake BioBank for Chinese (WBBC) Chinese. (b) Comparison between SG10K subpopulations and ChinaMAP Chinese or WBBC Chinese. (c) Comparison between ChinaMAP Chinese and WBBC Chinese. (d) Comparison between calculated carrier frequencies in gnomAD populations and actual ethnicity-specific carrier frequencies based on expanded carrier screening

Abbreviations: AFR=African or African-American, AMR=Hispanic (corresponding to Latino/Admixed American population in gnomAD), ASJ=Ashkenazi Jewish, EAS=East Asian, FCA=French Canadian or Cajun, FIN=Finnish, MEA=Middle Eastern, MWH=Mixed or Other White, NEU=Northern European, SAS=South Asian, SEA=Southeast Asian, SEU= Southern European

a comprehensive analysis of all known recessive genes. Our analysis pipeline can be readily adapted to prospective novel recessive genes. The overall number of androgen receptor genes with recognisable phenotypes is estimated to be between 9000 and 10 100, suggesting that currently known androgen receptor genes represent only approximately 20% of the total.

In an 18-month retrospective study of NBS for 24 inborn errors of metabolism in Hong Kong, where 86.5% of newborns are Chinese (East Asian) and the remaining are primarily Southeast or South Asian (Filipino, Indian, Nepalese, or Pakistani), nine patients with positivity for six inborn errors of metabolism were recorded. Carrier frequencies for these six diseases were particularly high in the East Asian and South Asian populations. Specifically, citrullinemia type II and carnitine uptake deficiency were confirmed in more than one Chinese patient, ranking 14th and 12th among carrier frequencies for all 2699 recessive genes in the WBBC cohort. Similarly, these two genes ranked 21st and 20th in the ChinaMAP cohort. Nevertheless, some of the remaining 18 diseases, for which no positive cases were identified, had low carrier frequency rates in both East and South Asian populations, indicating that more targeted selection for the region's NBS panel is warranted.

The design of NBS and ECS panels requires a careful balance between comprehensiveness and cost-effectiveness. Regarding NBS panels, only treatable diseases with relatively high prevalence should be included. Regarding ECS, as costs for next-generation sequencing decrease, increasing numbers of genes are added to various panels; there have been suggestions to include whole-exome sequencing or whole-genome sequencing in preconception carrier screening. However, larger panels reduce sequencing depth for individual genes, leading to missed variant calls. Moreover, these panels place unnecessary burdens on variant interpretation and genetic counselling, which are the most time- and cost-intensive processes. Therefore, genes and diseases included in NBS and ECS panels should be precisely selected and customised to the specific needs of each region or territory. Recent guidelines suggest a pan-ethnic, universal ECS panel for countries with mixed-race populations and a high likelihood of interracial couples. In countries and regions with a single majority ethnic group, a more focused panel would be more economically efficient and sufficient.

Conclusion

A robust pipeline was established to estimate and rank carrier frequencies; this pipeline is readily adaptable to new genome-wide sequencing data and prospective novel recessive genes. Because carrier frequencies in a given population constitute critical information for NBS and ECS design, our data-driven analysis provides a scientific basis and guidelines for such practices.

Funding

This study was supported by the Health and Medical Research Fund, Health Bureau, Hong Kong SAR Government (#08191216). The full report is available from the Health and Medical Research Fund website (https://rfs2.healthbureau.gov.hk).

Disclosure

The results of this research have been previously published in:

1. Zhu W, Wang C, Mullapudi N, et al. A robust pipeline for ranking carrier frequencies of autosomal recessive and X-linked Mendelian disorders. NPJ Genom Med 2022;7:72.

References

1. Guo MH, Gregg AR. Estimating yields of prenatal carrier screening and implications for design of expanded carrier screening panels. Genet Med 2019;21:1940-7.
2. Hanany M, Rivolta C, Sharon D. Worldwide carrier frequency and genetic prevalence of autosomal recessive inherited retinal diseases. Proc Natl Acad Sci U S A 2020;117:2710-6.
3. Tan J, Wagner M, Stenton SL, et al. Lifetime risk of autosomal recessive mitochondrial disorders calculated from genetic databases. EBioMedicine 2020;54:102730.
4. Haque IS, Lazarin GA, Kang HP, Evans EA, Goldberg JD, Wapner RJ. Modeled fetal risk of genetic diseases identified by expanded carrier screening. JAMA 2016;316:734-42.
5. Johansen Taber K, Ben-Shachar R, Torres R, et al. A guidelines-consistent carrier screening panel that supports equity across diverse populations. Genet Med 2022;24:201-13.

Add-on astragalus therapy for diabetic kidney disease: an open-label randomised controlled trial with responder regression analysis (abridged secondary publication)

KW Chan, ASK Kwong, PN Tsui, GCW Chan, WF Choi, WH Yiu, SCY Cheung, Y Zhang, MMY Wong, BJ Cowling, Z Zhang, KCB Tan, Y Feng, LX Lao, KN Lai, SCW Tang *

KEY MESSAGES

1. Add-on astragalus treatment for 48 weeks significantly improves kidney function in patients with stage 2 to 3 chronic diabetic kidney disease and macroalbuminuria.
2. The improvement occurs independently of blood pressure, blood glucose, and albuminuria control.

Hong Kong Med J 2025;31(Suppl 1):S19-22
HMRF project number: 14151731

[1] **KW Chan**, [2] **ASK Kwong**, [3] **PN Tsui**, [4] **GCW Chan**, [5] **WF Choi**, [1] **WH Yiu**, [6] **SCY Cheung**, [6] **Y Zhang**, [3] **MMY Wong**, [7] **BJ Cowling**, [6] **Z Zhang**, [8] **KCB Tan**, [6] **Y Feng**, [5,9] **LX Lao**, [1] **KN Lai**, [1] **SCW Tang**

[1] *Division of Nephrology, Department of Medicine, The University of Hong Kong, Hong Kong SAR, China*
[2] *Department of Family Medicine and Primary Healthcare, Hospital Authority Hong Kong West Cluster, Hong Kong SAR, China*
[3] *Department of Family Medicine and Primary Healthcare, Hospital Authority Hong Kong East Cluster, Hong Kong SAR, China*
[4] *Division of Nephrology, Department of Medicine, Queen Mary Hospital, Hong Kong SAR, China*
[5] *School of Chinese Medicine, The University of Hong Kong, Hong Kong SAR, China*
[6] *Department of Medicine, Queen Elizabeth Hospital, Hong Kong SAR, China*
[7] *School of Public Health, The University of Hong Kong, Hong Kong SAR, China*
[8] *Division of Endocrinology, Department of Medicine, The University of Hong Kong, Hong Kong SAR, China*
[9] *Virginia University of Integrative Medicine, Virginia, USA*

* Principal applicant and corresponding author: scwtang@hku.hk

Introduction

Diabetic kidney disease (DKD) is characterised by a progressive increase in albuminuria and/or a decline in renal function, as measured by glomerular filtration rate (GFR). DKD is the leading cause of end-stage kidney failure necessitating dialysis or transplantation. The pathogenesis of DKD is multifaceted. Conventional treatment strategies include control of blood pressure, blood glucose, and proteinuria. Traditional Chinese medicine (TCM) can further reduce the risk of end-stage kidney failure by 59%.[1] However, the effectiveness of TCM for DKD remains unclear.

Astragalus membranaceus, also known as huang-qi, is a frequently used TCM and dietary supplement for DKD. In a meta-analysis, astragalus more effectively improves renal clearance and reduces albuminuria than routine care; its effects are comparable to those of angiotensin-converting enzyme inhibitors or angiotensin receptor blockers.[2] In vivo and in vitro evidence suggests that astragaloside IV, an active ingredient of astragalus, can ameliorate podocyte apoptosis, foot process effacement, mesangial expansion, glomerulosclerosis, and interstitial fibrosis by regulating the NF-κB and TGF-β_1 signalling pathways. We previously showed that patients with DKD who received astragalus had a greater likelihood of response. We aimed to evaluate the effect of an add-on astragalus-based TCM in patients with stage 2 to 3 DKD and macroalbuminuria.

Methods

The READY clinical trial recruited 118 patients aged 35 to 80 years from six outpatient clinics and the community who had type 2 diabetes diagnosed at least 5 years prior, repeated estimated GFR of 30 to 90 mL/min/1.73 m^2 over 3 months, and persistent macroalbuminuria confirmed by a urine-to-creatinine ratio (UACR) of ≥34 mg/mmol, and were treated with stable doses of anti-diabetic medication (eg, insulin and angiotensin II receptor blockers/angiotensin-converting enzyme inhibitors) for 12 weeks. The participants were randomly assigned at a 1:1 ratio to receive either 48 weeks of add-on oral astragalus (<30 g/day) or standard medical care. The sample size was calculated based on the intention to control inflation factors for sample size estimation in subsequent studies.[3]

Primary outcomes were the slopes of changes in estimated GFR and UACR between baseline (week 0) and the treatment endpoint (week 48). Secondary outcomes included changes in blood pressure, biomarkers, and adverse events. Blood pressure was measured, and blood and urine samples were collected after an overnight fast (>8

hours). Biomarkers were assessed by an independent medical laboratory. Adverse events were recorded using a patient-completed questionnaire.

Outcomes were analysed using a mixed-effects regression model with an intention-to-treat approach. Hazard ratios for concomitant drug changes and major adverse events were estimated using a Cox proportional-hazards model, adjusted for baseline values of the corresponding outcome. Sensitivity analyses were conducted to test the robustness of the findings.

Results

In total, 118 patients with DKD were randomly assigned to receive either 48 weeks of add-on oral astragalus (n=56) or standard medical care (n=62). Baseline demographics were comparable between the two groups (Table). The mean age was 67.9 years, mean haemoglobin A1c was 7.0%, mean duration of diabetes was 13.4 years, mean estimated GFR was 58.0 mL/min/1.73 m^2, and mean UACR was 124.9 mg/mmol. The slope of estimated GFR decline was 4.58 mL/min/1.73 m^2 per year (95% confidence interval=1.53-7.63), with a smaller decline in astragalus-treated patients (-0.24±1.12 vs -4.16±1.07, P=0.003). Patients who received add-on astragalus had a 3.87 mL/min/1.73 m^2 (95% confidence interval=1.29-6.45) higher endpoint least-squares mean estimated GFR than the standard care controls (57.87 vs 54.00 mL/min/1.73 m^2, P=0.003). There was no significant change in UACR from baseline among astragalus-treated patients; the difference between groups was also not significant (Fig).

Compared with standard care controls, patients who received add-on astragalus had significantly lower systolic blood pressure and gamma-glutamyl transferase levels (although not clinically significant) and significantly higher levels of haemoglobin and urate. Levels of serum potassium, serum lipids, and liver enzymes were comparable between the two groups, as were the rates of hospitalisation and specialist referral, and serum levels of TNF-alpha, TNF receptor 1, TNF receptor 2, MCP-1, VEGF, and TGF-beta1 levels, as well as the urine MCP-1-to-creatinine ratio.

Three (5.4%) serious adverse events occurred in the astragalus group: one spontaneous death, one hospitalisation for pancreatitis with acidosis and acute kidney injury, and one hospitalisation for dyspnoea. In the standard care group, seven (11.3%) serious adverse events occurred: one ischaemic stroke, one hospitalisation for laryngeal obstruction by foreign body, one hospitalisation for hyperkalaemia, one hospitalisation for dyspnoea, one hospitalisation for palpitation, one hospitalisation for injurious fall, and one hospitalisation for hypertension. The difference in the number of serious adverse events between the two groups was not significant.

There were no significant pairwise interactions of treatment effect with age, sex, baseline DKD stage, baseline UACR level, or TCM subgroups. However, a trend toward a better response was observed among patients who were older, had earlier-stage DKD, or exhibited a lower UACR level at baseline. These results remained robust in all sensitivity analyses.

Discussion

Patients with stage 2 to 3 DKD and macroalbuminuria who received add-on astragalus had a significantly higher estimated GFR after 48 weeks, compared with patients who received standard care. The demographics of our cohort were comparable to those of other major trials (eg, DAPA-CKD, CREDENCE). The annual estimated GFR decline (-3.60 to -4.16 mL/min/1.73 m^2 in sensitivity analyses) observed in our standard care controls was consistent with declines recorded in DAPA-CKD (-4 mL/min/1.73 m^2) and CREDENCE (-5 mL/min/1.73 m^2), as well as our previous trial (-4.06 to -4.67 mL/min/1.73 m^2). The estimated GFR decline after add-on astragalus ranged from 1.21 to -0.24 mL/min/1.73 m^2, which is equivalent to the natural estimated GFR decline observed in healthy ageing or general populations. The estimated treatment effect was 4.58 (range, 4.25-5.39) mL/min/1.73 m^2. This magnitude of treatment effect has been associated with a 30% to 80% decrease in subsequent all-cause mortality in other DKD cohorts.[4] Therefore, the effect of astragalus in stabilising kidney function appears to be clinically significant.

Although there was no significant difference in albuminuria change between the two groups, a previous study of atrasentan showed possible kidney protection independent of albuminuria reduction. Nevertheless, analyses of systemic and kidney-specific inflammation- and fibrosis-related biomarkers did not reveal any significant differences. We hypothesise that putative targets of astragalus in DKD could involve the TNF signalling pathway, the hormonal system, and the renin-angiotensin system. Further analyses, including a systematic proteomics analysis, are warranted to delineate the underlying mechanisms of action.

There was minimal attrition in the astragalus group. Most attrition in the standard care group was caused by reluctance to attend follow-up appointments without receiving study medication. Further studies and implementation strategies should consider more user-friendly form of medication (eg, granules, tablets, capsules), decentralised investigation tools (eg, digital monitoring and home-based sampling), and cross-over designs using waitlists or placebo controls.

Our study had several limitations. First, it

TABLE. Patient characteristics at baseline

Variable	All patients (n=118)*	Add-on astragalus (n=56)*	Standard care (n=62)*	P value
Age, y	67.9±7.8	67.2±7.9	68.5±7.8	0.380
Female	43 (36.4)	20 (35.7)	23 (37.1)	0.876
Body mass index, kg/m^2	28.0±4.3	28.1±4.3	27.9±4.3	0.774
Haemoglobin A1c, %	7.0±1.0	7.1±0.9	7.0±1.1	0.753
History of diabetes, y	13.4±7.2	14.1±8.4	12.8±6.0	0.348
Smoking history				0.418
Non-smoker	76 (64.4)	33 (58.9)	43 (69.4)	
Ex-smoker	22 (18.6)	13 (23.2)	9 (14.5)	
Current smoker	20 (17.0)	10 (17.9)	10 (16.1)	
Smoking duration, y	12.0±18.9	14.1±19.7	10.0±18.1	0.236
Blood pressure, mmHg				
Systolic	152.1±19.0	153.3±20.8	151.1±17.3	0.538
Diastolic	77.0±10.0	76.4±10.6	77.5±9.4	0.548
Estimated glomerular filtration rate, mL/min/1.73 m^2	58.0±17.5	57.2±16.6	58.7±18.4	0.624
Urine albumin-to-creatinine ratio, mg/mmol	124.9±2.2	133.7±2.3	117.4±2.0	0.369
Urine albumin-to-creatinine ratio, mg/g	1105.3±19.5	1183.2±20.4	1038.9±17.7	0.369
Cholesterol, mmol/L				
Triglyceride	1.8±0.0	2.0±1.2	1.7±0.9	0.151
High-density lipoprotein	1.1±0.3	1.1±0.3	1.1±0.2	0.798
Low-density lipoprotein	2.5±0.7	2.5±0.6	2.5±0.7	0.904
Haemoglobin, g/dL	13.1±1.6	12.9±1.6	13.2±1.6	0.265
Serum potassium, mmol/L	4.6±0.4	4.6±0.4	4.6±0.4	0.943
Comorbidity				
Diabetic retinopathy	79 (67.0)	36 (64.3)	43 (69.4)	0.559
Coronary artery disease	5 (4.2)	1 (1.8)	4 (6.5)	0.209
History of stroke	7 (5.9)	5 (8.9)	2 (3.2)	0.190
Known peripheral artery disease	2 (1.7)	2 (3.6)	0	0.133
Congestive heart failure	0	0	0	-
Concomitant medication				
Angiotensin-converting enzyme inhibitors	52 (44.1)	21 (37.5)	31 (50)	0.172
Angiotensin receptor blockers	66 (55.9)	35 (62.5)	31 (50)	0.172
Maximally tolerated dose of the above drugs	103 (87.3)	50 (89.3)	53 (85.5)	0.536
Beta-blocker	49 (41.5)	20 (35.7)	29 (46.8)	0.223
Diuretic	15 (12.7)	7 (12.5)	8 (12.9)	0.948
Calcium channel blocker	99 (83.9)	46 (82.1)	53 (85.5)	0.622
Statin	92 (78.0)	46 (82.1)	46 (74.2)	0.298
Aspirin	16 (13.6)	7 (12.5)	9 (14.5)	0.749
Metformin	106 (89.8)	52 (92.9)	54 (87.1)	0.301
Sulfonylurea	68 (57.6)	28 (50.0)	40 (64.5)	0.111
Insulin	22 (18.6)	12 (21.4)	10 (16.1)	0.460
SGLT2i	15 (12.7)	8 (14.3)	7 (11.3)	0.626
DPP-4i	37 (31.4)	16 (28.6)	21 (33.9)	0.536
GLP-1 RA	4 (3.4)	4 (7.1)	0	0.032

* Data are presented as mean ± standard deviation or No. (%) of patients

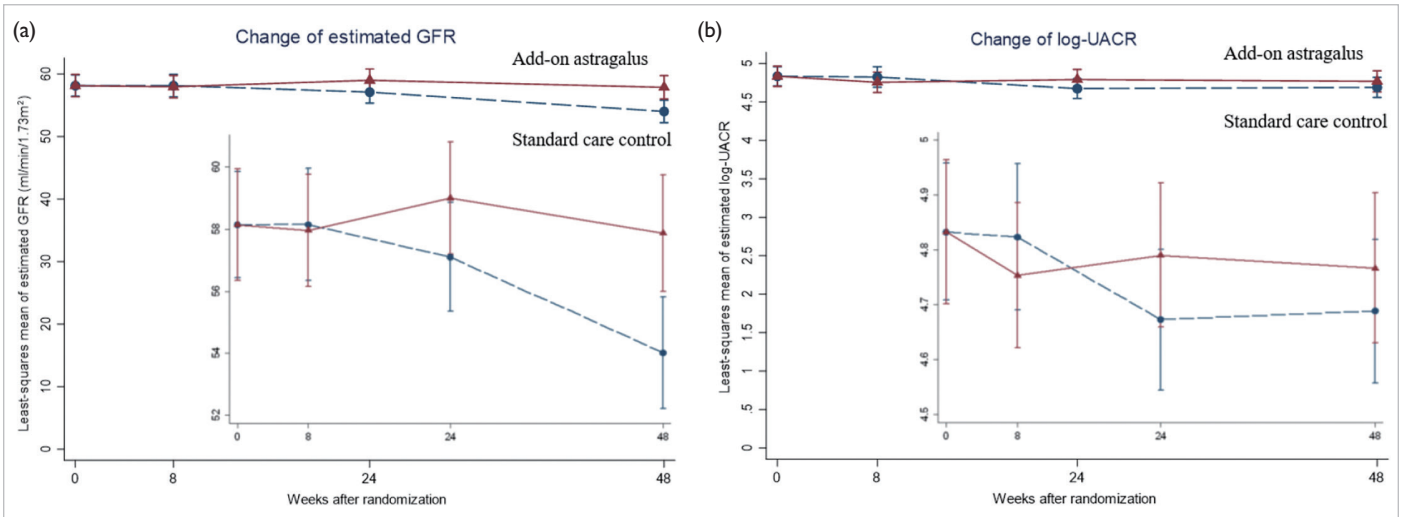

FIG. (a) The mixed-effects regression model with an intention-to-treat approach shows that the slope of estimated glomerular filtration rate (GFR) decline was 4.58 mL/min/1.73 m^2 per year (95% confidence interval=1.53-7.63), with a smaller decline in astragalus-treated patients (-0.24±1.12 vs -4.16±1.07, P=0.003). (b) There is no significant change in the urine albumin-to-creatinine ratio (UACR) from baseline among astragalus-treated patients, and the difference between the two groups was not significant

was not double-blind placebo-controlled because placebos are not routinely used in pragmatic trials and do not exert favourable clinical effect on continuous laboratory outcomes.[5] To minimise potential placebo effects, we assessed objective primary outcomes to reduce detection bias, adjusted for blood pressure control in sensitivity analyses, and analysed the intention-to-treat population via data tracking and sensitivity analyses on censoring criteria to decrease attrition bias. Second, our study had a relatively small sample size and short duration due to limited funding. We recruited patients with stage 2 to 3 DKD and macroalbuminuria who represent a more homogenous group with faster disease progression and are therefore more likely to benefit from add-on astragalus treatment. Nevertheless, large-scale trials are needed to determine the long-term effectiveness of astragalus treatment beyond 48 weeks.

Conclusion

Add-on astragalus treatment for 48 weeks significantly improved kidney function and thus could be a useful strategy in the multidisciplinary management of DKD. We recommend the inclusion of TCM for DKD in the public health system.

Funding

This study was supported by the Health and Medical Research Fund, Health Bureau, Hong Kong SAR Government (#14151731). The full report is available from the Health and Medical Research Fund website (https://rfs2.healthbureau.gov.hk).

Disclosure

The results of this research have been previously published in:

1. Chan KW, Kwong ASK, Tsui PN, et al. Add-on astragalus in type 2 diabetes and chronic kidney disease: a multi-center, assessor-blind, randomized controlled trial. Phytomedicine 2024;130:155457.

Acknowledgements

We thank C & H Medical Laboratory for sample analysis, Data and Safety Monitoring Board members for recommendations in study design, and PuraPharm for providing discounted medication.

References

1. Lin MY, Chiu YW, Chang JS, et al. Association of prescribed Chinese herbal medicine use with risk of end-stage renal disease in patients with chronic kidney disease. Kidney Int 2015;88:1365-73.
2. Liu Y, Tian H. Effect of astragalus membranaceus on diabetic nephropathy: a systematic review. Chin J Evid Based Med 2007;7:715-27.
3. Chan KW, Kwong ASK, Tsui PN, et al. Efficacy, safety and response predictors of adjuvant astragalus for diabetic kidney disease (READY): study protocol of an add-on, assessor-blind, parallel, pragmatic randomised controlled trial. BMJ Open 2021;11:e042686.
4. Turin TC, Coresh J, Tonelli M, et al. Change in the estimated glomerular filtration rate over time and risk of all-cause mortality. Kidney Int 2013;83:684-91.
5. Hróbjartsson A, Gøtzsche PC. Is the placebo powerless? An analysis of clinical trials comparing placebo with no treatment. N Engl J Med 2001;344:1594-602.

Self-administered acupressure for knee osteoarthritis: a randomised controlled trial (abridged secondary publication)

WF Yeung *, LX Lao, LKP Suen, JYS Ho, LM Ho, TC Chong, CK Wong, DST Cheung

KEY MESSAGES

1. Two 2-hour sessions of self-administered acupressure training was effective in alleviating knee pain and improving mobility in older adults with knee osteoarthritis.
2. Participants trained in self-administered acupressure reported significantly lower pain scores at weeks 4, 8, and 12, compared with participants receiving knee health education.
3. The self-administered acupressure training programme demonstrated high acceptability and compliance and was cost-effective.

Hong Kong Med J 2025;31(Suppl 1):S23-6
HMRF project number: 16172441

[1] WF Yeung, [2,3] LX Lao, [1] LKP Suen, [1] JYS Ho, [4] LM Ho, [5] TC Chong, [6] CK Wong, [7] DST Cheung

[1] *School of Nursing, The Hong Kong Polytechnic University, Hong Kong SAR, China*
[2] *School of Chinese Medicine, The University of Hong Kong, Hong Kong SAR, China*
[3] *Virginia University of Integrative Medicine, Virginia, USA*
[4] *School of Public Health, The University of Hong Kong, Hong Kong SAR, China*
[5] *TriO Health Sports and Spine Centre, Hong Kong SAR, China*
[6] *Department of Family Medicine and Primary Care, The University of Hong Kong, Hong Kong SAR, China*
[7] *School of Nursing, The University of Hong Kong, Hong Kong SAR, China*

* Principal applicant and corresponding author: jerry-wf.yeung@polyu.edu.hk

Introduction

Knee osteoarthritis (OA) affects 16% of people aged ≥45 years. It leads to reduced physical fitness and quality of life and increased healthcare utilisation. Acupuncture is an effective treatment for knee OA pain. Acupressure, a non-invasive variant, stimulates the same acupoints using fingers, hands, or elbows. We conducted a randomised controlled trial to evaluate the short- and medium-term effects of self-administered acupressure (SAA) on alleviating knee OA pain in older adults.

Methods

Between September 2019 and May 2022, older adults with knee OA were recruited to participate in either SAA training or knee health education (KHE). Participants attended two 2-hour sessions, held 1 week apart. They were instructed to practise SAA or follow KHE guidance nightly during the 12-week study period and to record their adherence in a logbook.

Participants were assessed at baseline, week 4, week 8, and week 12 by a single research assistant who was blinded to group allocation. The primary outcome measure was the numerical rating scale for pain ranging from 0 (no pain) to 10 (worst pain imaginable). Secondary outcome measures included the Western Ontario and McMaster University Osteoarthritis Index (WOMAC) subscales for pain, stiffness, and physical function; the Short-Form Six Dimensions (physical functioning, role limitations, social functioning, pain, mental health, and vitality); the timed up and go test; and gait speed.

Results

In total, 314 participants were randomly assigned to receive either SAA (n=157) or KHE (n=157) [Table 1]. All participants attended all sessions; they reported high willingness to attend similar training courses, with scores of 9.5 and 9.3, respectively. Of the 146 participants in the SAA group who returned their logbooks, 116 performed acupressure at least 4 days per week throughout the 12-week period. The mean duration of self-practice at home was 16.5 minutes per day.

Compared with the KHE group, the SAA group reported lower pain scores at week 4 (P<0.01), week 8 (P<0.01), and week 12 (P=0.015) [Table 2]. The SAA group also performed better in the timed up and go test at week 8 (P=0.03) but not at week 12. Additionally, the SAA group exhibited greater improvement in Short-Form Six Dimensions scores at week 12 (P=0.03).

The quality-adjusted life year, as measured by Short-Form Six Dimensions scores from baseline to week 12, in the SAA group was 0.1651, which was 0.0042 higher than the 0.1609 observed in the KHE group. However, this difference was not significant (P=0.101). The mean cost of the SAA training per participant was higher than KHE (HK$698 vs HK$652, P=0.002). The incremental cost-effectiveness ratio for SAA in knee OA was

TABLE 1. Baseline characteristics of participants

Variable	All (n=314)*	Self-administered acupressure (n=157)*	Knee health education (n=157)*	P value
Age, y	62.7±4.54	62.6±4.72	62.8±4.36	0.710
Women	246 (78.3)	123 (78.3)	123 (78.3)	1.000
Education level				0.798
Primary or below	28 (8.9)	14 (8.9)	14 (8.9)	
Secondary 1-3	60 (19.1)	32 (20.4)	28 (17.8)	
Secondary 4-7	122 (38.9)	63 (40.1)	59 (37.6)	
Degree or above	104 (33.1)	48 (30.6)	56 (35.7)	
Marital status†				0.911
Single	40 (12.8)	19 (12.2)	21 (13.5)	
Cohabitation	14 (4.5)	8 (5.1)	6 (3.8)	
Married	222 (71.2)	113 (72.4)	109 (69.9)	
Divorced	19 (6.1)	8 (5.1)	11 (7.1)	
Widowed	17 (5.4)	8 (5.1)	9 (5.8)	
Employment status				0.397
Professional/semi-professional	31 (9.9)	18 (11.5)	13 (8.3)	
Skilled worker	17 (5.4)	9 (5.7)	8 (5.1)	
Non-skilled worker	7 (2.2)	2 (1.3)	5 (3.2)	
Retired	169 (53.8)	82 (52.2)	87 (55.4)	
Housewife	69 (22)	35 (22.3)	34 (21.7)	
Unemployed	8 (2.5)	2 (1.3)	6 (3.8)	
Others	13 (4.1)	9 (5.7)	4 (2.5)	
Body mass index, kg/m²	23.5±2.87	23.4±2.91	23.5±2.84	0.793
Presence of health problem	220 (70.1)	120 (76.4)	100 (63.7)	0.014
Knee pain duration, mo	7.3±7.58	7.5±7.02	7.1±8.13	0.584
Current use of painkillers for knee pain	43 (13.7)	20 (12.7)	23 (14.6)	0.622
Previous knee osteoarthritis management				
Western medicine	140 (44.6)	76 (48.4)	64 (40.8)	0.173
Physiotherapy	119 (37.9)	56 (35.7)	63 (40.1)	0.415
Chinese medicine (internal use)	42 (13.4)	22 (14)	20 (12.7)	0.740
Chinese medicine (external use)	55 (17.5)	25 (15.9)	30 (19.1)	0.458
Supplements	218 (69.4)	109 (69.4)	109 (69.4)	1.000

* Data are presented as mean ± standard deviation or No. (%) of participants
† Missing data of two participants

HK$10 873.6. A non-parametric cost-effectiveness acceptability curve indicated a 80% probability that SAA would be cost-effective at a willingness-to-pay threshold of HK$44 000, and >90% probability at a threshold equivalent to one gross domestic product per capita (Fig).

Discussion

A brief SAA training, combined with a short KHE session, effectively alleviates knee pain in older adults with knee OA. SAA outperformed KHE in alleviating knee pain throughout the 12-week study period. Participants in the SAA group demonstrated significantly better performance in the timed up and go test and achieved a higher quality of life at week 8. The high acceptability and compliance observed in the SAA group further support its feasibility. However, SAA did not result in a significantly greater quality-adjusted life year improvement. Nevertheless, SAA remains a cost-effective intervention.

SAA training led to significant improvements in knee pain. Although both groups exhibited reductions in WOMAC scores, no significant between-group difference was observed. This finding is consistent with a previous study that

TABLE 2. Comparison of outcomes between groups across four timepoints

Outcome	Self-administered acupressure (n=157)*	Knee health education (n=157)*	Between-group difference in change (95% confidence interval)	Effect size	P value
Numerical rating scale for pain					
Baseline	5.140±0.151	5.146±0.154	-	-	-
Week 4	3.742±0.153	4.333±0.156	-0.585 (-0.96 to -0.21)	0.35	0.002
Week 8	3.436±0.156	4.105±0.158	-0.662 (-1.08 to -0.24)	0.35	0.002
Week 12	3.034±0.156	3.575±0.154	-0.535 (-0.97 to -0.10)	0.27	0.015
Western Ontario and McMaster University Osteoarthritis Index					
Pain					
Baseline	6.822±0.260	7.586±0.276	-	-	-
Week 4	5.655±0.264	6.638±0.278	-0.219 (-0.81 to 0.37)	0.08	0.464
Week 8	5.068±0.268	6.237±0.280	-0.404 (-1.09 to 0.28)	0.13	0.246
Week 12	5.031±0.267	5.859±0.281	-0.064 (-0.78 to 0.65)	0.02	0.860
Stiffness					
Baseline	2.497±0.127	2.987±0.133	-	-	-
Week 4	2.022±0.129	2.651±0.134	-0.138 (-0.46 to 0.18)	0.10	0.396
Week 8	1.886±0.131	2.302±0.135	0.075 (-0.28 to 0.43)	0.05	0.677
Week 12	1.914±0.131	2.216±0.135	0.188 (-0.17 to 0.55)	0.12	0.295
Physical function					
Baseline	21.924±0.907	25.376±0.978	-	-	-
Week 4	18.546±0.919	21.501±0.982	0.497 (-1.33 to 2.32)	0.06	0.593
Week 8	16.291±0.930	20.067±0.989	-0.323 (-2.49 to 1.85)	0.03	0.773
Week 12	16.168±0.931	19.250±0.994	0.371 (-1.92 to 2.66)	0.04	0.749
Timed up and go test, s					
Baseline	10.781±0.155	10.992±0.148	-	-	-
Week 4	9.791±0.165	10.361±0.154	-0.358 (-0.73 to 0.02)	0.21	0.053
Week 8	9.337±0.173	10.014±0.162	-0.466 (-0.88 to -0.05)	0.25	0.030
Week 12	9.483±0.169	9.765±0.161	-0.069 (-0.48 to 0.34)	0.04	0.737
Gait speed, m/s					
Baseline	3.833±0.077	3.809±0.058	-	-	-
Week 4	3.906±0.085	3.802±0.06	0.08 (-0.13 to 0.29)	0.08	0.494
Week 8	3.849±0.091	3.826±0.063	-0.001 (-0.22 to 0.21)	0.00	0.928
Week 12	3.674±0.088	3.722±0.062	-0.071 (-0.28 to 0.14)	0.07	0.523
Short Form-Six Dimension					
Baseline	0.691±0.009	0.685±0.009	-	-	-
Week 4	0.714±0.009	0.700±0.009	0.008 (-0.01 to 0.03)	0.08	0.459
Week 8	0.724±0.009	0.702±0.009	0.017 (-0.01 to 0.04)	0.15	0.164
Week 12	0.739±0.009	0.707±0.009	0.027 (0.00 to 0.05)	0.24	0.030

* Data are presented as mean ± standard error

demonstrated significant improvements in pain scores for both verum SAA and sham SAA groups compared with usual care.[1] However, verum SAA significantly reduced WOMAC pain and function scores compared with usual care, which contrasts with the results of the present study. This discrepancy may be attributed to differences in the comparison groups; the present study used KHE as a comparator. Decreasing trends were observed in knee pain, WOMAC scores for pain, stiffness, and functional limitations, as well as in the timed up and go test for both groups from baseline to post-intervention.

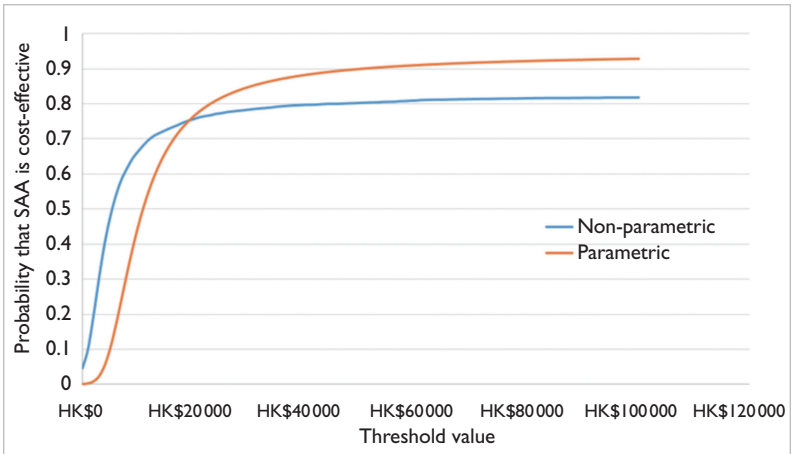

FIG. Cost-effectiveness acceptability curves of self-administered acupressure for knee osteoarthritis

The use of KHE as a comparator avoided differences in contact time between the instructor and participants relative to SAA training. Any observed improvement in pain may be partially related to non-specific effects arising from this interaction. In contrast, care-as-usual or waitlist controls do not adjust for such non-specific effects and may inadvertently induce nocebo effects due to the perception of 'not being treated'.[2] The use of sham controls in acupuncture-related trials remains contentious because the characteristics of the intervention itself may contribute to non-specific treatment effects.[3] These effects are not always readily distinguishable. Accordingly, the present study utilised KHE of equivalent duration to standardise contact hours between the instructor and participants.

SAA is a reliable and well-tolerated non-pharmacological intervention.[4] The most frequently reported adverse effect is finger joint pain, which may result from prolonged pressing of acupoints using fingers or improper techniques.[5] Other reported adverse effects include pain or bruising at the stimulation sites, pricking pain sensations in the legs, and muscle spasms. Most adverse effects are mild, self-resolving, and preventable with proper acupressure techniques to minimise finger overuse or by using acupressure rods.

The present study had several limitations. First, the absence of a sham control group limited the ability to distinguish the specific effects of SAA. Second, the lack of objective measures to assess knee swelling or range of motion may weaken the validity of the study outcomes. Third, participants in the KHE group may have performed SAA, leading to potential underestimation of the treatment effect size.

Conclusion

A brief SAA training, combined with a short KHE session, effectively alleviated knee pain in older adults with knee OA. Participants exhibited high acceptability and compliance with the SAA programme. SAA remains a cost-effective intervention although it did not result in a significantly greater quality-adjusted life year.

Funding

This study was supported by the Health and Medical Research Fund, Health Bureau, Hong Kong SAR Government (#16172441). The full report is available from the Health and Medical Research Fund website (https://rfs2.healthbureau.gov.hk).

Disclosure

The results of this research have been previously published in:

1. Yeung WF, Chen SC, Cheung DST, et al. Self-administered acupressure for probable knee osteoarthritis in middle-aged and older adults: a randomized clinical trial. JAMA Netw Open 2024;7:e245830.

Acknowledgements

We thank Dr Lau Chi-Ling, Dr Lin Wai-Ling, and Mr Chung Wai-Yeung for facilitating the SAA training. We also thank Ms Chan Ying-Tung, Ms Sing-Fung Ng, and Ms Fong Ka-Na for conducting the knee health education sessions.

References

1. Li LW, Harris RE, Tsodikov A, Struble L, Murphy SL. Self-acupressure for older adults with symptomatic knee osteoarthritis: a randomized controlled trial. Arthritis Care Res (Hoboken) 2018;70:221-9.
2. Paterson C, Dieppe P. Characteristic and incidental (placebo) effects in complex interventions such as acupuncture. BMJ 2005;330:1202-5.
3. Chen H, Ning Z, Lam WL, et al. Types of control in acupuncture clinical trials might affect the conclusion of the trials: a review of acupuncture on pain management. J Acupunct Meridian Stud 2016;9:227-33.
4. Yeung WF, Chung KF, Poon MMK, et al. Acupressure, reflexology, and auricular acupressure for insomnia: a systematic review of randomized controlled trials. Sleep Med 2012;13:971-84.
5. Zhang Y, Shen CL, Peck K, et al. Training self-administered acupressure exercise among postmenopausal women with osteoarthritic knee pain: a feasibility study and lessons learned. Evid Based Complement Alternat Med 2012;2012:570431.

Acupuncture for insomnia in patients with breast cancer undergoing chemotherapy: a randomised sham-controlled trial (abridged secondary publication)

J Zhang, Z Qin, TH So, TY Chang, S Yang, H Chen, WF Yeung, KF Chung, PY Chan, LX Lao, ZJ Zhang *

KEY MESSAGES

1. Insomnia is a highly prevalent symptom during and after chemotherapy.
2. Acupuncture was not superior to the sham control in reducing the Insomnia Severity Index score from baseline to 6 weeks (mean difference= -0.4, P=0.609). However, it achieved superior short-term and long-term outcomes in improving sleep onset latency, total sleep time, sleep efficiency, anxiety, depression, and quality of life. The acupuncture group exhibited a higher cessation rate of sleeping medication use (56.5% vs 14.3%, P=0.011).
3. Acupuncture could be considered for the management of chemotherapy-associated insomnia and for tapering or replacing sleeping medications in patients with breast cancer.

Hong Kong Med J 2025;31(Suppl 1):S27-31
HMRF project number: 16172761

[1,2] J Zhang, [1] Z Qin, [3] TH So, [4] TY Chang, [1] S Yang, [1] H Chen, [5] WF Yeung, [6] KF Chung, [1] PY Chan, [1,7] LX Lao, [1,8] ZJ Zhang

[1] *School of Chinese Medicine, The University of Hong Kong, Hong Kong SAR, China*
[2] *Hong Kong Chinese Medicine Clinical Study Centre, School of Chinese Medicine, Hong Kong Baptist University, Hong Kong SAR, China*
[3] *Department of Clinical Oncology, LKS Faculty of Medicine, The University of Hong Kong, Hong Kong SAR, China*
[4] *Comprehensive Oncology Centre, Hong Kong Sanatorium & Hospital, Hong Kong SAR, China*
[5] *School of Nursing, The Hong Kong Polytechnic University, Hong Kong SAR, China*
[6] *Department of Psychiatry, The University of Hong Kong, Hong Kong SAR, China*
[7] *Virginia University of Integrative Medicine, Virginia, USA*
[8] *Department of Chinese Medicine, The University of Hong Kong Shenzhen Hospital, Shenzhen, Guangdong, China*

* Principal applicant and corresponding author: zhangzj@hku.hk

Introduction

More than one-fourth of patients with breast cancer experience insomnia during chemotherapy. Insomnia increases the risks of psychiatric and physical comorbidities and reduces patients' willingness to complete treatment. This study aimed to evaluate the efficacy and safety of acupuncture for chemotherapy-associated insomnia in patients with breast cancer.

Methods

Women aged 18 to 75 years with a diagnosis of stage I-IV breast cancer who were undergoing or had completed chemotherapy within the past 6 months and had insomnia were invited to participate. Insomnia was defined as occurring at least 3 nights per week and persisting for >1 month, based on the diagnostic criteria for brief insomnia disorder in the Diagnostic and Statistical Manual of Mental Disorders (5th Edition). The Insomnia Severity Index (ISI) score was required to be at least 10 over the past 2 weeks. Patients were excluded if they had other sleep disorders, irregular sleep patterns or shift work; severe hearing, visual, or language impairments; severe haematological dysfunction; pacemakers or other electronic implants that could interfere with electroacupuncture; acupuncture treatment within the past 3 months; or participation in other clinical trials within the past 3 months.

Permuted block randomisation was used. Investigators and participants were blinded to group allocation. Acupuncture treatments were administered by registered Chinese medicine practitioners with at least 5 years of clinical practice experience. Participants received 15 treatment sessions; 12 sessions were provided twice weekly over 6 consecutive weeks as intensive treatment, and then three sessions were provided once every 4 weeks between weeks 7 and 18 to maintain treatment effects. Participants were followed up between weeks 19 and 42.

The active acupuncture regimen consisted of electroacupuncture at body acupoints and auricular acupressure. Six acupoints (EX-HN1, GV20, GV24, PC6, KI3, and SP6) were selected for insomnia treatment. Four additional acupoints were used to address comorbid symptoms. Auricular acupressure involved embedding hard, black *Vaccaria* seeds on the surfaces of three bilateral auricular points (Heart, Shenmen, and Sympathetic).

Sham acupuncture was performed at points located 1 to 2 cm adjacent to the meridian-based acupoints. Streitberger non-invasive retractable needles were used. Sham auricular acupressure was performed at points in the helix region (HX7, HX8, HX9). Soft stem piths of Medulla Junci were used to

TABLE 1. Characteristics of participants

Characteristic	Active acupuncture (n=69)*	Sham acupuncture (n=69)*	Total (n=138)*
Age, y	51.7±9.6	52.7±8.3	52.2±9.0
Body mass index, kg/m2	22.8±2.9	24.0±16.9	23.4±12.1
Marital status			
Married or living with partner	48 (69.6)	45 (65.2)	93 (67.4)
Single, separated, divorced, or widowed	21 (30.4)	24 (34.8)	45 (32.6)
Education level			
Primary or below	7 (10.1)	8 (11.6)	15 (10.9)
Secondary	33 (47.8)	33 (47.8)	66 (47.8)
Post-secondary or above	29 (42.0)	28 (40.6)	57 (41.3)
Household monthly income, HK$			
<20 000	36 (52.2)	39 (56.5)	75 (54.3)
20 000-50 000	23 (33.3)	13 (18.8)	36 (26.1)
>50 000	10 (14.5)	15 (21.7)	25 (18.1)
No answer	0	2 (2.9)	2 (1.4)
Occupation			
Professional and associate professional	22 (31.9)	20 (29.0)	42 (30.4)
Skilled and semi-skilled worker	3 (4.3)	3 (4.3)	6 (4.3)
Unskilled worker	19 (27.5)	12 (17.4)	31 (22.5)
Retired/unemployed/housework	25 (36.2)	34 (49.3)	59 (42.8)
Menopausal status			
Premenopausal	4 (5.8)	1 (1.4)	5 (3.6)
Perimenopausal	13 (18.8)	13 (18.8)	26 (18.8)
Postmenopausal	52 (75.4)	55 (79.7)	107 (77.5)
Breast cancer stage			
I	13 (18.8)	19 (27.5)	32 (23.2)
II	29 (42.0)	26 (37.7)	55 (39.9)
III	15 (21.7)	17 (24.6)	32 (23.2)
IV	10 (14.5)	7 (10.1)	17 (12.3)
No answer	2 (2.9)	0	2 (1.4)
Prior surgery	61 (88.4)	64 (92.8)	125 (90.6)
Prior radiotherapy	37 (53.6)	40 (58.0)	77 (55.8)
Prior hormonal therapy	34 (49.3)	38 (55.1)	72 (52.2)
Adjuvant chemotherapy	51 (73.9)	57 (82.6)	108 (78.3)
Chemotherapy			
In progress	15 (21.7)	17 (24.6)	32 (23.2)
Post	54 (78.3)	52 (75.4)	72 (52.2)
Chemotherapy regimens			
Adriamycin and cyclophosphamide, or docetaxel and cyclophosphamide	14 (20.3)	20 (29.0)	34 (24.6)
Docetaxel, adriamycin, and cyclophosphamide	6 (8.7)	10 (14.5)	16 (11.6)
Adriamycin and cyclophosphamide, or epirubicin and cyclophosphamide + docetaxel or paclitaxel	13 (18.8)	9 (13.0)	22 (15.9)
Fluorouracil, epirubicin and cyclophosphamide + docetaxel	8 (11.6)	5 (7.2)	13 (9.4)
Carboplatin-containing	17 (24.6)	14 (20.3)	31 (22.5)
Others	11 (15.9)	11 (15.9)	22 (15.9)
Insomnia duration, mo	9.0 (3.0-13.5)	10.0 (5.5-15.0)	9.0 (4.8-14.0)
Sleep aids, prior 2 weeks			
Sleep medications	26 (37.7)	19 (27.5)	45 (32.6)
Chinese herbal medicine	16 (23.2)	24 (34.8)	40 (29.0)
Prior acupuncture	50 (72.5)	46 (66.7)	96 (69.6)
Insomnia Severity Index	17.4±4.3	16.7±4.5	17.1±4.4
Pittsburgh Sleep Quality Index	13.6±3.4	12.7±3.3	13.1±3.4
Actiwatch			
Sleep onset latency, min	14.2±14.5	14.2±12.3	14.2±13.4
Wake after sleep onset, min	112.6±40.2	112.5±38.4	112.5±39.2
Total sleep time, min	359.1±51.1	357.7±51.3	358.4±51.0
Sleep efficiency, %	72.8±7.9	72.9±7.5	72.8±7.7
Sleep diary			
Sleep onset latency, min	51.5±38.6	47.8±35.7	49.6±37.1
Wake after sleep onset, min	58.0±44.0	56.2±47.1	57.1±45.4
Total sleep time, min	319.4±85.2	331.1±96.8	325.3±91.1
Sleep efficiency, %	64.8±15.4	68.2±17.9	66.5±16.8
Hospital Anxiety and Depression Scale			
Anxiety	9.2±3.9	8.6±3.2	8.9±3.6
Depression	8.4±4.1	8.1±3.8	8.3±3.9
Brief Fatigue Inventory	5.6±2.1	5.6±2.1	5.6±2.1
Brief Fatigue Inventory-Short Form			
Pain severity	3.4±2.9	4.3±2.4	3.9±2.7
Pain interference	3.3±3.1	3.9±2.7	3.6±2.9
Functional Assessment of Cancer Therapy-Breast Cancer	80.3±21.3	82.5±19.7	81.4±20.4
Acupuncture Expectancy Scale	14.8±3.4	14.8±3.3	14.8±3.3

* Data are presented as mean ± standard deviation or No. (%) of participants

mimic auricular acupressure.

The primary outcome was the change in ISI score from baseline to 6 weeks of treatment. Secondary outcomes included sleep measures (Actiwatch recordings, sleep diaries, and the Pittsburgh Sleep Quality Index), depression and anxiety (measured using the Hospital Anxiety and

Depression Scale), fatigue (measured using the Brief Fatigue Inventory), pain (measured using the Brief Pain Inventory-Short Form), and quality of life (measured using the Functional Assessment of Cancer Therapy-Breast Cancer).

The proportion of participants prescribed sleeping medications was recorded, along with the dosage and weekly frequency of use. The dosage was standardised by conversion to diazepam-equivalent dosages. Four mean dosages were calculated by averaging values across 2-week periods at four time points (prior to study entry, post-treatment 6 and 18 weeks, and before the end of follow-up).[1] The cessation rate of sleeping medication use was determined.

Based on a previous study involving participants with an ISI score difference of 2.5 and a pooled standard deviation of 4.7,[2] a sample size of 138 participants was required to achieve a 95% level of significance and 80% power, assuming a 20% dropout rate. Efficacy was analysed according to the intention-to-treat principle. Missing data were handled using the multiple imputation method under the missing-at-random assumption. Comparisons were made using a mixed-effects model adjusted for baseline values, time, group, and their interaction.

Results

Of 415 patients screened, 166 were eligible, but 28 declined to participate. The remaining 138 participants were randomly assigned to receive either active acupuncture (n=69) or sham acupuncture (n=69). Among these, 15 (10.9%) participants discontinued within the first 6 weeks, and 23 (16.7%) discontinued before trial completion. The active acupuncture group had a lower discontinuation rate (8.7% vs 24.6%, P=0.012) and a higher rate of completing at least 12 treatments (97.1% vs 81.2%). The two groups were comparable in terms of baseline characteristics (Table 1).

The active acupuncture group demonstrated a higher cessation rate of sleeping medication use during weeks 18 to 20, compared with the sham control group (56.5% vs 14.3%, P=0.011). However, the two groups did not differ significantly in dosage of sleeping medications and weekly frequency of use.

Both groups showed a reduction in ISI scores from baseline over the 42-week study period (P<0.001) but did not differ significantly at any measurement point (Table 2). Both groups experienced significant improvements from baseline in sleep quality, wake time after sleep onset, anxiety, depression, fatigue, pain, and quality of life (P<0.05 for all). At week 6, active acupuncture was more effective than sham control in shortening sleep onset latency, as measured by Actiwatch (P<0.001) and sleep diary (P=0.044); increasing total sleep time, as measured by sleep diary (P<0.001); and improving sleep efficiency, as measured by Actiwatch (P=0.049) and sleep diary (P=0.005). However, the two groups did not differ significantly in changes in Pittsburgh Sleep Quality Index. The active acupuncture group showed a greater reduction in anxiety at week 10 (P=0.016) and in both anxiety and depression at week 42 (P≤0.001), as well as greater improvement in quality of life at week 14 (P=0.024) and week 42 (P<0.001).

Treatment-related adverse effects were mild. Two serious adverse effects unrelated to treatment (pneumonia) were reported in the active acupuncture group. The most common adverse effect was bruising (n=6). Four participants in the sham acupuncture group experienced auricular skin allergic reactions. No participants discontinued treatment due to adverse effects.

Discussion

Compared with the sham acupuncture group, the active acupuncture group demonstrated significantly greater improvements in sleep onset latency, total sleep time, and sleep efficiency. However, the two groups did not differ significantly in changes in ISI scores or the Pittsburgh Sleep Quality Index. This discrepancy may be because (1) the short-term efficacy of acupuncture in alleviating insomnia is more apparent than its long-term efficacy, and (2) the Actiwatch and sleep diary exhibit greater sensitivity in detecting insomnia improvements compared with other measures.

Our sham control group showed a greater improvement in ISI scores at 6 weeks, compared with other sham-controlled acupuncture trials. This may have contributed to the smaller effect size and the lack of significant differences between groups. Nonetheless, the active acupuncture group experienced greater reductions in anxiety and depression and greater improvements in quality of life during both treatment and follow-up periods. Additionally, during weeks 18 to 20, a greater proportion of participants in the active acupuncture group discontinued the use of sleeping medications. The present study had several limitations. First, Streitberger placebo needles may have exerted modulatory effects on multiple levels of the central nervous system by stimulating mechanoreceptors beneath the skin. Second, the active acupuncture regimen included both acupuncture at body acupoints and auricular acupressure. It remains unclear whether the beneficial effects arose from the two acupuncture modes acting individually or synergistically. Finally, the Actiwatch was the only objective measure used; discrepancies were observed between Actiwatch and sleep diary results. Additional objective measures such as polysomnography are needed to validate the findings from Actiwatch and clinical instruments.

TABLE 2. Comparisons of changes in outcomes from baseline between and within groups

Outcome	Change from baseline*		Between-group difference*	P value
	Active acupuncture (n=69)	Sham acupuncture (n=69)		
Insomnia Severity Index				
Week 3	-4.4 (-5.4 to -3.5)†	-3.6 (-4.6 to -2.6)†	-0.8 (-2.2 to 0.6)	0.265
Week 6	-5.9 (-6.9 to -4.9)†	-5.5 (-6.6 to -4.5)†	-0.4 (-1.8 to 1.1)	0.609
Week 10	-6.5 (-7.5 to -5.5)†	-6.6 (-7.6 to -5.5)†	0.1 (-1.4 to 1.6)	0.894
Week 14	-7.0 (-7.9 to -6.0)†	-6.7 (-7.8 to -5.6)†	-0.2 (-1.7 to 1.2)	0.736
Week 18	-7.6 (-8.6 to -6.6)†	-7.2 (-8.2 to -6.1)†	-0.5 (-1.9 to 1.0)	0.541
Week 30	-6.8 (-7.8 to -5.8)†	-5.9 (-7.0 to -4.8)†	-0.9 (-2.3 to 0.6)	0.249
Week 42	-7.5 (-8.5 to -6.5)†	-6.7 (-7.7 to -5.6)†	-0.8 (-2.3 to 0.6)	0.265
Actiwatch at week 6				
Sleep onset latency, min	-7.5 (-9.8 to -5.3)†	1.5 (-0.9 to 3.9)	-9.0 (-12.3 to -5.7)	<0.001
Wake after sleep onset, min	-7.2 (-12.1 to -2.4)†	-8.2 (-13.5 to -2.9)†	1.0 (-6.2 to 8.2)	0.784
Total sleep time, min	2.7 (-4.2 to 9.6)	2.3 (-5.3 to 9.9)	0.4 (-9.8 to 10.6)	0.943
Sleep efficiency, %	2.8 (1.8 to 3.8)†	1.3 (0.3 to 2.4)	1.5 (0.0 to 2.9)	0.049
Sleep diary at week 6				
Sleep onset latency, min	-11.4 (-18.9 to -3.9)†	-3.3 (-11.1 to 4.6)	-8.1 (-16.1 to -0.2)	0.044
Wake after sleep onset, min	-9.2 (-16.2 to 2.2)	-13.5 (-21.2 to -5.8)†	4.3 (-6.1 to 14.8)	0.413
Total sleep time, min	42.8 (32.2 to 53.3)†	13.5 (1.9 to 25.1)	29.2 (13.5 to 44.9)	<0.001
Sleep efficiency, %	8.6 (6.5 to 10.6)†	4.1 (1.8 to 6.4)†	4.4 (1.3 to 7.5)	0.005
Pittsburgh Sleep Quality Index				
Week 3	-2.3 (-3.0 to -1.5)†	-2.1 (-2.9 to -1.4)†	-0.1 (-1.2 to 0.9)	0.808
Week 6	-3.4 (-4.2 to -2.7)†	-3.3 (-4.2 to -2.5)†	-0.1 (-1.2 to 1.0)	0.894
Week 10	-4.1 (-4.8 to -3.3)†	-3.9 (-4.7 to -3.1)†	-0.2 (-1.3 to 0.9)	0.742
Week 14	-4.6 (-5.3 to -3.8)†	-3.7 (-4.5 to -2.9)†	-0.9 (-2.0 to 0.2)	0.123
Week 18	-5.0 (-5.7 to -4.2)†	-4.5 (-5.3 to -3.7)†	-0.5 (-1.6 to 0.7)	0.408
Week 30	-4.9 (-5.6 to -4.1)†	-4.0 (-4.9 to -3.2)†	-0.8 (-2.0 to 0.3)	0.148
Week 42	-5.2 (-6.0 to -4.4)†	-4.2 (-5.0 to -3.3)†	-1.0 (-2.1 to 0.1)	0.084
Hospital Anxiety and Depression Scale				
Anxiety				
Week 3	-1.0 (-1.6 to -0.4)†	-0.5 (-1.1 to 0.1)	-0.5 (-1.3 to 0.3)	0.250
Week 6	-2.0 (-2.5 to -1.4)†	-1.2 (-1.9 to -0.6)†	-0.7 (-1.6 to 0.1)	0.098
Week 10	-2.1 (-2.7 to -1.5)†	-1.0 (-1.7 to -0.4)†	-1.1 (-1.9 to -0.2)	0.016
Week 14	-1.9 (-2.5 to -1.3)†	-1.3 (-2.0 to -0.7)†	-0.6 (-1.4 to 0.3)	0.213
Week 18	-2.3 (-2.9 to -1.7)†	-1.8 (-2.4 to -1.1)†	-0.5 (-1.4 to 0.4)	0.256
Week 30	-2.1 (-2.7 to -1.5)†	-1.8 (-2.5 to -1.2)†	-0.2 (-1.1 to 0.6)	0.593
Week 42	-2.6 (-3.2 to -2.0)†	-1.0 (-1.7 to -0.4)†	-1.6 (-2.4 to -0.7)	0.001
Depression				
Week 3	-0.7 (-1.4 to -0.1)†	-0.8 (-1.5 to -0.1)†	-0.1 (-0.9 to 1.0)	0.889
Week 6	-1.3 (-1.9 to -0.6)†	-1.5 (-2.2 to -0.8)†	0.2 (-0.7 to 1.2)	0.613
Week 10	-2.0 (-2.6 to -1.3)†	-1.5 (-2.2 to -0.8)†	-0.5 (-1.4 to 0.5)	0.354
Week 14	-2.1 (-2.8 to -1.5)†	-1.7 (-2.4 to -1.0)†	-0.4 (-1.4 to 0.5)	0.382
Week 18	-2.2 (-2.9 to -1.6)†	-2.2 (-2.9 to -1.5)†	-0.0 (-1.0 to 0.9)	0.932
Week 30	-2.1 (-2.8 to -1.5)†	-1.5 (-2.3 to -0.8)†	-0.6 (-1.6 to 0.4)	0.227
Week 42	-3.2 (-3.9 to -2.5)†	-1.3 (-2.0 to -0.6)†	-1.9 (-2.9 to -0.9)	< .001
Brief Fatigue Inventory				
Week 3	-1.0 (-1.5 to -0.6)†	-1.1 (-1.5 to -0.6)†	0.0 (-0.6 to 0.7)	0.917
Week 6	-1.7 (-2.2 to -1.3)†	-1.7 (-2.2 to -1.2)†	-0.0 (-0.7 to 0.6)	0.907
Week 10	-2.1 (-2.6 to -1.7)†	-1.6 (-2.1 to -1.1)†	-0.5 (-1.2 to 0.1)	0.117
Week 14	-2.5 (-2.9 to -2.0)†	-2.1 (-2.6 to -1.6)†	-0.4 (-1.0 to 0.3)	0.261
Week 18	-2.6 (-3.1 to -2.2)†	-2.2 (-2.7 to -1.7)†	-0.4 (-1.1 to 0.2)	0.189
Week 30	-2.4 (-2.9 to -2.0)†	-1.9 (-2.4 to -1.4)†	-0.5 (-1.2 to 0.1)	0.110
Week 42	-2.7 (-3.2 to -2.2)†	-2.1 (-2.6 to -1.6)†	-0.5 (-1.2 to 0.2)	0.134

* Data are presented as mean (95% confidence interval)

† Adjusted P<0.05

TABLE 2. (cont'd)

Outcome	Change from baseline*		Between-group difference*	P value
	Active acupuncture (n=69)	Sham acupuncture (n=69)		
Brief Fatigue Inventory-Short Form				
Pain severity				
Week 3	-0.7 (-1.2 to -0.2)†	-0.5 (-1.0 to 0.0)†	0.2 (-0.9 to 0.5)	0.578
Week 6	-0.6 (-1.1 to -0.1)	-0.6 (-1.2 to -0.1)†	0.0 (-0.7 to 0.8)	0.914
Week 10	-1.0 (-1.5 to -0.5)†	-1.2 (-1.7 to -0.6)†	0.2 (-0.6 to 0.9)	0.642
Week 14	-1.0 (-1.4 to -0.5)†	-1.0 (-1.5 to -0.5)†	0.0 (-0.7 to 0.8)	0.917
Week 18	-0.7 (-1.2 to -0.2)	-1.2 (-1.7 to -0.6)†	0.4 (-0.3 to 1.2)	0.232
Week 30	-1.0 (-1.5 to -0.5)†	-1.2 (-1.8 to -0.7)†	0.3 (-0.5 to 1.0)	0.470
Week 42	-1.1 (-1.6 to -0.6)†	-0.7 (-1.2 to -0.2)†	0.4 (-1.1 to 0.4)	0.285
Pain interference				
Week 3	-0.8 (-1.3 to -0.3)†	-0.5 (-1.0 to 0.0)†	-0.3 (-1.0 to 0.4)	0.375
Week 6	-0.9 (-1.4 to -0.4)	-0.8 (-1.3 to -0.3)†	-0.1 (-0.8 to 0.6)	0.817
Week 10	-1.2 (-1.7 to -0.7)†	-1.0 (-1.5 to -0.5)†	-0.2 (-0.9 to 0.5)	0.528
Week 14	-1.5 (-2.0 to -1.0)†	-1.3 (-1.8 to -0.8)†	-0.2 (-0.9 to 0.5)	0.530
Week 18	-1.2 (-1.7 to -0.7)†	-1.5 (-2.1 to -1.0)†	0.4 (-0.4 to 1.1)	0.331
Week 30	-1.2 (-1.7 to -0.7)†	-1.6 (-2.1 to -1.1)†	0.4 (-0.3 to 1.1)	0.300
Week 42	-1.6 (-2.1 to -1.1)†	-1.2 (-1.7 to -0.6)†	-0.5 (-1.2 to 0.3)	0.210
Functional Assessment of Cancer Therapy-Breast Cancer				
Week 3	6.3 (3.3 to 9.4)†	6.8 (3.6 to 10.0)†	-0.4 (-4.9 to 4.0)	0.842
Week 6	10.6 (7.5 to 13.7)†	9.8 (6.5 to 13.1)†	0.8 (-3.8 to 5.3)	0.742
Week 10	14.2 (11.1 to 17.3)†	10.5 (7.1 to 13.9)†	3.7 (-0.9 to 8.3)	0.118
Week 14	14.7 (11.6 to 17.9)†	9.4 (6.0 to 12.8)†	5.3 (0.7 to 9.9)	0.024
Week 18	15.8 (12.6 to 18.9)†	12.3 (8.9 to 15.7)†	3.5 (-1.2 to 8.1)	0.141
Week 30	14.4 (11.3 to 17.6)†	12.6 (9.2 to 16.0)†	1.8 (-2.8 to 6.5)	0.441
Week 42	19.1 (15.9 to 22.3)†	10.1 (6.6 to 13.5)†	9.0 (4.3 to 13.7)	<0.001

Conclusion

The active acupuncture regimen could be considered for the management of chemotherapy-associated insomnia. It has the potential to taper and even replace the use of sleeping medications in patients with breast cancer.

Funding

This study was supported by the Health and Medical Research Fund, Health Bureau, Hong Kong SAR Government (#16172761). The full report is available from the Health and Medical Research Fund website (https://rfs2.healthbureau.gov.hk).

Disclosure

The results of this research have been previously published in:

1. Zhang J, Qin Z, So TH, et al. Acupuncture for chemotherapy-associated insomnia in breast cancer patients: an assessor-participant blinded, randomized, sham-controlled trial. Breast Cancer Res 2023;25:49.
2. Zhang J, Yang M, So TH, et al. Electroacupuncture plus auricular acupressure on chemotherapy-related insomnia in patients with breast cancer (EACRI): Study protocol for a randomized, sham-controlled trial. Integr Cancer Ther 2021;20:15347354211058695.
3. Zhang J, Zhang Z, Huang S, et al. Acupuncture for cancer-related insomnia: a systematic review and meta-analysis. Phytomedicine 2022;102:154160.

References

1. Zitman FG, Couvée JE. Chronic benzodiazepine use in general practice patients with depression: an evaluation of controlled treatment and taper-off: report on behalf of the Dutch Chronic Benzodiazepine Working Group. Br J Psychiatry 2001;178:317-24.
2. Yeung WF, Chung KF, Zhang SP, Yap TG, Law AC. Electroacupuncture for primary insomnia: a randomized controlled trial. Sleep 2009;32:1039-47.

Tele-delivered supportive cancer care for breast cancer survivors: abridged secondary publication

NCY Yeung *, EYY Chan, C Cheng, WWS Mak, JYM Siu, PSY Cheung

KEY MESSAGES

1. Among breast cancer survivors, 55% to 65% reported moderate-to-high intention to use various tele-delivered supportive cancer care (SCC) services including psychosocial care, complementary care, peer support, and medical consultation.
2. Higher intention to use different types of tele-delivered SCC was associated with performance expectancy, social influence, effort expectancy, facilitating conditions, unmet psychological needs, and unmet patient care and support needs.
3. Participants with higher intention to use tele-delivered SCC reported more favourable perceptions of telehealth than those with lower intention.

Hong Kong Med J 2025;31(Suppl 1):S32-7
HMRF project number: 18190061

[1] NCY Yeung, [1] EYY Chan, [2] C Cheng, [3] WWS Mak, [4] JYM Siu, [5] PSY Cheung

[1] *The Jockey Club School of Public Health and Primary Care, The Chinese University of Hong Kong, Hong Kong SAR, China*
[2] *Department of Psychology, The University of Hong Kong, Hong Kong SAR, China*
[3] *Department of Psychology, The Chinese University of Hong Kong, Hong Kong SAR, China*
[4] *Department of Applied Social Sciences, Hong Kong Polytechnic University, Hong Kong SAR, China*
[5] *Hong Kong Breast Cancer Foundation, Hong Kong SAR, China*

* Principal applicant and corresponding author: nelsoneyeung@cuhk.edu.hk

Introduction

The COVID-19 pandemic has impacted supportive cancer care (SCC) services for breast cancer survivors in Hong Kong. Telehealth offers an alternative means for delivering SCC during the pandemic.[1] This study aimed to assess the acceptability of tele-delivered SCC services (including psychosocial care, medical consultation, complementary care, and peer support) among breast cancer survivors in Hong Kong during the pandemic. We also evaluated how telehealth-related perceptions, multiple domains of unmet supportive care needs, and fear of COVID-19 were associated with intention to use tele-delivered SCC. Using a mixed-methods design based on the Unified Theory of Acceptance and Use of Technology,[2] this study provided quantitative and qualitative findings for comprehensive understanding of factors associated with intention to use tele-delivered SCC.

Methods

Between June and December 2022, Cantonese-speaking breast cancer survivors diagnosed at stages 0-III since the outbreak of COVID-19 (January 2020) were recruited from the Hong Kong Breast Cancer Registry. In phase 1, 209 eligible breast cancer survivors completed a cross-sectional survey in home settings; 30 of them (10 at each level of intention to use tele-delivered SCC [low, moderate, high]) were invited to participate in phase II qualitative interviews at the Hong Kong Breast Cancer Foundation or on Zoom. Participants received HK$100 and HK$300 supermarket coupons as compensation in phases I and II, respectively.

Outcome measures included telehealth perceptions (ie, performance expectancy, effort expectancy, social influence, facilitating conditions, and technology anxiety), unmet supportive care needs, fear of COVID-19, and sociodemographic/cancer-related variables. The interviews explored how these factors affected participants' intention to use tele-delivered SCC.

Variables with a P value of ≤0.05 in univariate regression models were entered into multivariate logistic regression models. Intention scores of ≥3 indicated moderate-to-high intention, whereas scores of 1 or 2 indicated low intention.

Interview transcripts were thematically analysed. Two coders independently coded each transcript, generating subthemes and themes through line-by-line content analysis. Discrepancies were resolved by consensus.

Results

Most breast cancer survivors reported moderate-to-high intention to use tele-delivered SCC: 55% for psychosocial care, complementary care, and peer support, and 65% for medical consultation (Table 1).

In univariate logistic regression, higher intention to use all four types of tele-delivered SCC were associated with performance expectancy, effort expectancy, social influence, and facilitating conditions (Table 2). Specifically, technology anxiety

was associated with lower intention to use tele-delivered medical consultation and complementary care. Greater unmet needs in the psychological, health system/information, and patient care/support domains were associated with higher intention to use tele-delivered medical consultation. Greater unmet psychological needs were also associated with higher intention to use tele-delivered psychosocial care.

In multivariate logistic regression, higher intention to use all four types of tele-delivered SCC remained associated with performance expectancy (odds ratio [OR]=1.66, P<0.05) and social influence (OR=4.64, P<0.01) [Table 2]. Specifically, effort expectancy was associated with higher intention to use tele-delivered medical consultation (OR=1.69, P<0.05). Facilitating conditions were associated with higher intention to use tele-delivered peer support (OR=1.87, P<0.01). Unmet psychological needs and patient care and support needs (OR=1.02, P<0.05) were associated with higher intention to use tele-delivered medical consultation.

Higher performance expectancy, effort expectancy, social influence, and facilitating conditions were associated with higher intention to use tele-delivered SCC. Qualitative findings were largely consistent with the quantitative results (Table 3), indicating that participants with higher intention to use tele-delivered SCC perceived more favourable telehealth perceptions, compared with participants with lower intention. Technology anxiety was the least-mentioned telehealth perception.

Participants with high intention to use tele-delivered SCC generally believed that telehealth was useful (performance expectancy) and easy to use (effort expectancy). Some noted the importance of access to appropriate devices (facilitating conditions) and support from others (social influence) when using tele-delivered SCC.

Participants with moderate intention to use tele-delivered SCC preferred face-to-face SCC but considered tele-delivered SCC helpful (performance expectancy) and easy to use (effort expectancy). However, some reported difficulties in using tele-delivered SCC without appropriate devices and access to the services (facilitating conditions). Support and recommendations from healthcare providers (social influence) could facilitate intention to use tele-delivered SCC.

Participants with lower intention to use tele-delivered SCC had lower performance expectancy and effort expectancy and less favourable facilitating conditions. Despite recommendations from close contacts (social influence) about tele-delivered SCC, some participants had insufficient resources and relevant knowledge (facilitating conditions) to use tele-delivered SCC.

Most unmet supportive care needs were not associated with intention to use tele-delivered SCC. Regardless of intention levels, participants generally experienced pain and physical limitations after breast cancer treatments (physical needs). They reported long waiting times and shorter-than-expected medical treatment durations in public hospitals (patient care and support needs), expressed a need to manage their emotions due to fear of recurrence (psychological needs), and encountered a lack of information about recovery and follow-ups (health system and information needs). Needs related to sexuality issues were also expressed.

Fear of COVID-19 was not associated with intention to use tele-delivered SCC (Table 3). Participants reporting high and moderate intention to use tele-delivered SCC expressed fear of contracting COVID-19 and considered telehealth an acceptable alternative. However, one participant with low intention to use tele-delivered SCC perceived a low level of fear of COVID-19 due to strict measures in public hospitals.

TABLE 1. Acceptability of tele-delivered supportive cancer care (SCC) among breast cancer survivors (n=209)

Tele-delivered SCC	No. (%) of participants with moderate or high intention to use SCC
Psychosocial care	
Psychotherapy	117 (56.0)
Psychological counselling and support	119 (56.9)
Psycho-oncology counselling	140 (67.0)
Therapist-led group sessions	133 (63.6)
Counselling for adjustment for cancer survivors and family members	113 (54.0)
Family counselling	71 (34.0)
Medical consultation	
Cancer helpline	130 (62.2)
Specialist medical consultation	132 (63.1)
Second opinion on treatment options	128 (61.2)
Palliative care consultation	129 (61.7)
Expert consultation	126 (60.3)
Nutrition consultation	165 (78.9)
Complementary/alternative/Chinese medicine consultation	139 (66.5)
Complementary care	
Movement and exercise activities (eg, yoga, qi gong, exercises for pain relief)	146 (69.9)
Creative therapies (music and art therapy)	105 (50.2)
Relaxation/breathing/meditation group sessions	121 (57.9)
Mindfulness exercises	103 (49.2)
Massage therapy	108 (51.7)
Peer support groups	
Internet forum with peers	95 (45.5)
Patient support group	131 (62.6)

TABLE 2. Variables associated with moderate-to-high intention to use tele-delivered supportive cancer care

Variables	Mean ± standard deviation	Odds ratio (95% confidence interval)	P value	Adjusted odds ratio (95% confidence interval)	P value
Tele-delivered psychosocial care					
Performance expectancy	3.65±0.65	4.87 (2.68-8.88)	<0.001	3.56 (1.74-7.28)	0.001
Effort expectancy	3.50±0.77	2.16 (1.42-3.30)	<0.001	1.14 (0.64-2.02)	0.66
Facilitating conditions	3.40±0.85	2.10 (1.43-3.09)	<0.001	1.09 (0.66-1.8)	0.74
Social influence	3.13±0.72	2.62 (1.65-4.16)	<0.001	3.42 (1.83-6.39)	0.00
Technology anxiety	2.38±0.75	0.71 (0.48-1.06)	0.09	-	-
Health system and information needs	40.42±27.28	1.01 (1.00-1.02)	0.19	-	-
Psychological needs	36.66±22.21	1.02 (1.00-1.03)	0.014	1.01 (0.99-1.02)	0.42
Physical needs	33.56±22.55	1.01 (0.99-1.02)	0.35	-	-
Patient care and support needs	36.34±26.20	1.01 (1.00-1.02)	0.16	-	-
Sexuality needs	18.98±22.81	1.01 (1.00-1.02)	0.11	-	-
Fear of COVID-19	2.55±0.70	1.10 (0.74-1.66)	0.64	-	-
Tele-delivered medical consultation					
Performance expectancy	3.65±0.65	2.16 (1.45-3.23)	<0.001	4.64 (2.50-8.62)	<0.001
Effort expectancy	3.50±0.77	2.16 (1.45-3.23)	<0.001	1.69 (1.06-2.70)	0.03
Facilitating conditions	3.40±0.85	1.98 (1.38-2.84)	<0.001	1.49 (0.98-2.27)	0.06
Social influence	3.13±0.72	2.66 (1.68-4.20)	<0.001	3.06 (1.82-5.13)	0.001
Technology anxiety	2.38±0.75	0.61 (0.41-0.89)	0.01	0.75 (0.49-1.17)	0.21
Health system and information needs	40.42±27.28	1.01 (1.00-1.03)	0.007	1.02 (1.01-1.03)	0.003
Psychological needs	36.66±22.21	1.02 (1.00-1.03)	0.02	1.02 (1.00-1.03)	0.02
Physical needs	33.56±22.55	1.01 (0.99-1.02)	0.38	-	
Patient care and support needs	36.34±26.20	1.02 (1.01-1.03)	0.002	1.02 (1.01-1.03)	0.001
Sexuality needs	18.98±22.81	1.01 (1.00-1.03)	0.056	-	
Fear of COVID-19	2.55±0.70	0.92 (0.62-1.36)	0.671	-	
Tele-delivered complementary care					
Performance expectancy	3.65±0.65	3.22 (1.90-5.45)	<0.001	3.07 (1.76-5.36)	<0.001
Effort expectancy	3.50±0.77	1.98 (1.32-2.98)	0.001	1.52 (0.97-2.49)	0.67
Facilitating conditions	3.40±0.85	1.48 (1.05-2.10)	0.03	1.07 (0.69-1.65)	0.76
Social influence	3.13±0.72	1.91 (1.24-2.92)	0.003	1.79 (1.15-2.79)	0.01
Technology anxiety	2.38±0.75	0.64 (0.43-0.95)	0.03	0.82 (0.53-1.28)	0.38
Health system and information needs	40.42±27.28	1.00 (0.99-1.01)	0.73	-	-
Psychological needs	36.66±22.21	1.00 (1.00-1.02)	0.25	-	-
Physical needs	33.56±22.55	1.01 (0.99-1.02)	0.48	-	-
Patient care and support needs	36.34±26.20	1.01 (1.00-1.02)	0.10	-	-
Sexuality needs	18.98±22.81	1.00 (0.99-1.01)	0.93	-	-
Fear of COVID-19	2.55±0.70	0.94 (0.63-1.40)	0.76	-	-
Tele-delivered peer support					
Performance expectancy	3.65±0.65	2.61 (1.61-4.23)	<0.001	2.16 (1.30-3.56)	0.003
Effort expectancy	3.50±0.77	1.86 (1.26-2.75)	0.002	1.31 (0.84-2.06)	0.23
Facilitating conditions	3.40±0.85	2.43 (1.65-3.58)	0.00	1.87 (1.19-2.94)	0.01
Social influence	3.13±0.72	1.68 (1.12-2.51)	0.012	1.66 (1.08-2.55)	0.02
Technology anxiety	2.38±0.75	0.69 (0.47-1.01)	0.06	-	-
Health system and information needs	40.42±27.28	1.00 (0.99-1.01)	0.42	-	-
Psychological needs	36.66±22.21	1.01 (1.00-1.03)	0.58	-	-
Physical needs	33.56±22.55	1.01 (1.00-1.02)	0.18	-	-
Patient care and support needs	36.34±26.20	1.01 (1.00-1.02)	0.23	-	-
Sexuality needs	18.98±22.81	1.01 (1.00-1.02)	0.16	-	-
Fear of COVID-19	2.55±0.70	1.32 (0.89-1.95)	0.17	-	-

TABLE 3. Exemplary quotes regarding telehealth perceptions, supportive care needs, and fear of COVID-19 (n=30)

Exemplary quote
Telehealth perceptions
Performance expectancy
"Telehealth helps a lot when I am not able to walk comfortably during treatment. It is convenient; we can use the service anytime and anywhere." (P36, high intention)
"It is handy when I do not want to go out and feel unwell." (P58, high intention)
"I prefer seeing the doctor or attending a class in person. Face to face would be best; they can know and understand your current situation, but during the pandemic, using telehealth is still good." (P4, moderate intention)
"I like using telehealth to meet with doctors as it is convenient and saves time on transportation and waiting." (P8, moderate intention)
"There are limitations with telehealth for Chinese medicine consultations. Doctors can't touch and observe the patients clearly during telehealth sessions." (P62, low intention)
"I think telehealth can't help breast cancer patients much." (P6, low intention)
"I sometimes get lymphedema, itches, and rashes on my body, which need doctors to check physically. I really can't imagine how telehealth could address that." (P42, low intention)
Effort expectancy
"It is easy to revisit the content with video recording." (P60, high intention)
"It would be easy once you master the skills." (P13, high intention)
"If we are willing to learn, it wouldn't be difficult." (P54, high intention)
"It is easy to use. Just click on the link you sent me." (P8, moderate intention)
"It is clearer to use video calls to describe my symptoms and understand instructions from doctors by seeing their facial expressions. However, it is harder to communicate by phone calls." (P38, moderate intention)
"I feel I have put much effort into those group sessions, but it is easy to miss things when I am not fully focused." (P42, low intention)
Facilitating conditions
"With the help of others' instructions, I have adapted to telehealth software." (P36, high intention)
"Having a mobile phone and laptop, I don't find it very challenging." (P59, high intention)
"People will likely use telehealth if they know how to use it." (P15, high intention)
"I only have a phone, not an iPad or devices with a larger screen. The screen is too small for me, but it is not too hard to use telehealth." (P7, moderate intention)
"It is hard to express my feelings clearly in front of the device." (P43, moderate intention)
"Telehealth services also require reservations, and the quotas are limited." (P4, moderate intention)
"My family members and healthcare workers suggested that I use telehealth, but you need Wi-Fi. I didn't have Wi-Fi at home before… so I was not willing to use it." (P26, low intention)
"I haven't tried it yet because I don't know new technology well." (P33, low intention)
"I only have a phone for telehealth, not an iPad, and the screen on my phone is too small for me." (P14, low intention)
Social influence
"Nurses from the non-governmental organisation encouraged me to download Zoom as the clinic visit service was cancelled." (P13, high intention)
"Nurses from the hospital encouraged me to join a support group meeting on Zoom before the next visit, so that I would know what to expect when I meet the doctor again." (P4, moderate intention)
"I didn't know how to make an appointment in telehealth at first. After the staff helped me download the app and taught me how to use it, I found it was not hard to use." (P25, moderate intention)
Technology anxiety
"I feel nervous about not knowing how to use it." (P7, moderate intention)
"I am nervous about mistakenly pressing the wrong button on telehealth platforms." (P8, moderate intention)
"At first, I was worried that I didn't know how to use Zoom with its different functions such as raising my hand, connecting with video and audio, but I felt better after learning it." (P13, high intention)
Supportive care needs
Physical needs
"My physical strength and skin conditions have worsened." (P59, high intention)
"I am not able to carry heavy things." (P29, moderate intention)
"The medicines definitely have side effects; I sleep poorly after taking them." (P62, low intention)

TABLE 3. (cont'd)

Exemplary quote
Psychological needs
"The chance of recurrence makes me worried." (P36, high intention)
"I am worried that it will spread to other parts of my body." (P3, moderate intention)
"After getting cancer, you are scared that it might happen again." (P6, low intention)
Patient care & support needs
"In public hospitals, especially for us, we have to wait from morning until night to see the doctor, and we can't ask many questions." (P13, high intention)
"The doctor at the private hospital made me angry; he answered my questions casually and didn't care much about me." (P3; moderate intention)
Heath system & information needs
"I would like a full body check after the treatments, but I don't know relevant information, like how or where to check." (P13, high intention)
"I think I need information about nutrition and diet after surgery, what exercises I should do, etc." (P8; moderate intention)
"There is no follow-up, like a PET scan after radiotherapy. How can I know if the treatment is effective?" (P43, low intention)
Sexuality needs
"We do not have sex after my surgery because my husband is so scared; he doesn't dare to look at it." (P13, high intention)
"I get nervous when changing clothes. I don't want my husband to see my scars." (P7; moderate intention)
"Sometimes when my husband kisses my left breast, he smells something like ointment… he doesn't want to kiss anymore." (P14, low intention)
COVID-19 perception
Fear of Covid-19
"Besides going to the hospital… I don't go out, because I am very scared of getting infected. Through this Zoom session, chatting with other cancer patients, I feel there's some support… otherwise, it would like total isolation from the outside world." (P58, high intention)
"I feel safe from infection by joining the services remotely during the pandemic." (P7, moderate intention)
"I'm not scared… there are fewer people in the hospitals during the pandemic… they won't let you in without checking you thoroughly; you don't need to be scared." (P33, low intention)

Discussion

Among breast cancer survivors during the COVID-19 pandemic, 55% to 65% reported moderate-to-high intention to use different types of tele-delivered SCC. Our findings are consistent with the acceptability of telemedicine in approximately 60% of Singaporean cancer patients during the pandemic.[4] Higher education level and confidence in using technological devices were associated with higher intention to use tele-delivered SCC. These findings are consistent with those reported from Western countries, suggesting cultural or geographical universality.

Most variables based on the Unified Theory of Acceptance and Use of Technology were associated with intention to use tele-delivered SCC. The importance of performance expectancy was highlighted. Based on the qualitative findings, participants with high intention to use tele-delivered SCC tended to view telehealth as convenient, efficient, time-saving, and useful. Emphasising these benefits in daily living may increase intention to use.[5]

Social influence was associated with intention to use tele-delivered SCC. In Chinese culture, family opinions are crucial for cancer patients' treatment decisions and psychosocial care. During the pandemic, online consultations and support programmes facilitated non-co-residential family members to participate. Chinese people value healthcare workers' recommendations. Greater support from close contacts and healthcare workers increased the acceptance of tele-delivered SCC. Future interventions should more effectively involve family members in cancer patients' SCC.

Facilitating conditions were associated with intention to use tele-delivered psychosocial care and peer support, whereas effort expectancy was not associated with intention to use tele-delivered peer support. Chinese breast cancer survivors rarely utilise psychological care and peer support groups. Open disclosure of personal challenges in counselling or support groups may conflict with the cultural preference to avoid showing negative emotions in front of others. Despite finding telehealth easy to use (high effort expectancy), breast cancer survivors still considered that they needed more knowledge, preparation, or courage before joining

tele-delivered psychosocial care and support groups. This was echoed by a participant who noted that a lack of personal space in the family environment was a barrier to participating in certain tele-delivered psychosocial or peer support services.

Unmet supportive care needs did not differ significantly across participants with different levels of intention to use tele-delivered SCC. However, unmet psychological needs and patient care and support needs were associated with higher intention to use tele-delivered medical consultation. During the pandemic, breast cancer survivors commonly experienced long waiting times, shorter-than-expected medical consultation durations, and a lack of timely support from healthcare staff (patient care and support needs), as well as concerns about recurrence (psychological needs). Considering that telehealth might offer more timely care, patients reporting greater unmet psychological and patient care and support needs may be more receptive to tele-delivered medical consultation.

The role of fear of COVID-19 in facilitating intention to use tele-delivered SCC was inconsistent between quantitative and qualitative findings. This may be due to the scale used to measure fear of COVID-19, which primarily captured participants' affective responses to COVID-19-related cues rather than their perceived risk of contracting COVID-19 in social settings. Greater specificity in measuring fear of COVID-19, threats, or concerns may improve the ability to explain intention to use tele-delivered SCC.

This study had some limitations. First, we recruited voluntary breast cancer survivors through a single registry, which might not represent all breast cancer survivors in Hong Kong and potentially limiting the generalisability of the findings. Second, not all variables associated with intention to use tele-delivered SCC were investigated. Other variables (eg, characteristics of tele-delivered SCC and contextual factors such as pandemic situations) could have been associated.[5] Healthcare professionals should recognise the importance of enhancing telehealth skills, promoting positive perceptions of telehealth, and addressing specific supportive care needs that facilitate the use of tele-delivered SCC, particularly during future pandemics. For breast cancer survivors who are older, of lower socioeconomic status, or not confident in using technological devices, digital literacy programmes and assistance in accessing technological devices may enhance intention to use tele-delivered SCC.

Funding

This study was supported by the Health and Medical Research Fund, Health Bureau, Hong Kong SAR Government (#18190061). The full report is available from the Health and Medical Research Fund website (https://rfs2.healthbureau.gov.hk).

Disclosure

The results of this research have been previously published in:

1. Yeung NCY, Lau STY, Mak WWS, et al. Applying the unified theory of acceptance and use of technology to identify factors associated with intention to use teledelivered supportive care among recently diagnosed breast cancer survivors during COVID-19 in Hong Kong: Cross-sectional survey. JMIR Cancer 2024;10:e51072.

References

1. Breastcancer.org. Special Report: COVID-19's impact on breast cancer care 2020. Accessed 11 July 2024. Available from: https://www.breastcancer.org/treatment/covid-19-and-breast-cancer-care#breastcancer.
2. Dwivedi YK, Rana NP, Jeyaraj A, et al. Re-examining the Unified Theory of Acceptance and Use of Technology (UTAUT): towards a revised theoretical model. Inf Syst Front 2019;21:719-34.
3. Zhang Y, Liu C, Luo S, et al. Factors influencing patients' intentions to use diabetes management apps based on an extended Unified Theory of Acceptance and Use of Technology model: web-based survey. J Med Internet Res 2019;21:e15023.
4. Chan ZY, Lim CF, Leow JL, et al. Using the technology acceptance model to examine acceptance of telemedicine by cancer patients in an ambulatory care setting. Proc Singapore Healthc 2022;31. doi:20101058221104578.
5. Gajarawala SN, Pelkowski JN. Telehealth benefits and barriers. J Nurse Pract 2021;17:218-21.

Identification of new allergens in *Periplaneta americana* by omics and immunological techniques for cockroach-related allergic diseases: abridged secondary publication

WNS Au, TF Leung, KWS Tsui *

KEY MESSAGES

1. A high-quality, chromosome-level genome of Periplaneta americana was assembled and well-annotated, with a size of 3.06 Gb and 29 939 predicted protein-coding genes.
2. In silico identification of putative allergens was performed in the high-quality P americana genome, revealing a complete allergen profile that includes 43 allergen groups.
3. Proteomic analysis using immunoassay and mass spectrometry methods detected seven novel allergen groups: Per a 14, Per a 15, Per a 16, Per a 17, Per a 18, Per a 19, and Per a 20.
4. A new isoallergen of tropomyosin (Per a 7.02) and multiple potential isoallergens of Per a 5 were identified through bioinformatics and proteomic techniques.

Hong Kong Med J 2025;31(Suppl 1):S38-40
HMRF project number: 07181266

[1] WNS Au, [2] TF Leung, [3] KWS Tsui

[1] *School of Life Sciences, The Chinese University of Hong Kong, Hong Kong SAR, China*
[2] *Department of Paediatrics, The Chinese University of Hong Kong, Hong Kong SAR, China*
[3] *School of Biomedical Sciences, The Chinese University of Hong Kong, Hong Kong SAR, China*

* Principal applicant and corresponding author: kwtsui@cuhk.edu.hk

Introduction

The American cockroach (*Periplaneta americana*) is linked to allergic diseases. The degree of cockroach infestation is associated with the incidence of cockroach allergy in inner-city areas, leading to an increased risk of asthma onset and higher morbidity among asthmatic individuals.[1] The prevalences of cockroach allergy are 17% to 41% in the United States, 55% to 79% in Brazil, and 44% to 60% in Thailand. Cockroach allergens are detectable in their saliva, debris, secretions, and shed skin[2]; 23 allergens have been identified in the American cockroach and are divided into 13 groups (Per a 1-13). Despite increasing awareness of the negative impact and health implications of cockroach allergies, advances in diagnosis and treatment remain slow owing to the lack of a comprehensive cockroach allergen profile.

Methods

Samples of 8-month-old male and female adult *P americana* were raised. Paired-end sequencing of 150 bp gDNA was performed. A high-molecular-weight gDNA library was prepared and sequenced. Chicago and Hi-C libraries were constructed and sequenced. The backbone of the American cockroach genome was de novo assembled and polished. The final assembly was refined to chromosome level by scaffolding with Chicago and Hi-C data. Quality control was conducted.

The allergenic potential of annotated *P americana* proteins was evaluated based on amino acid sequence similarity with known allergens, mRNA expression levels, and the presence of T cell and B cell epitopes.

Skin prick tests were performed using a commercialised American cockroach extract and other common allergens. Individuals were asked to abstain from anti-allergy drugs for at least 7 days before testing. Histamine (2.5 mg/mL) served as a positive control; buffered saline solution constituted a negative control. Individuals with symptoms and positive results were recruited as cockroach-allergic patients, whereas healthy individuals with negative results were recruited as controls.

A crude protein extract of *P americana* was purified. Potential allergens in 43 gel spots were identified. The DNA sequences of eight potential allergens were retrieved from the genome and manually curated with support from transcriptomic reads. Start and stop codons, as well as exact exon-intron sites of each potential candidate, were identified to produce genes containing full-length sequences. To minimise mis-assembly, curated gene sequences were translated into amino acid sequences and searched against databases. Plasmid cloning, recombinant protein expression, and protein purification were performed. The allergenicity characteristics of the eight purified recombinant proteins were examined by enzyme-linked immunosorbent assay (ELISA).

Results

To de novo assemble the *P americana* genome, 129.3 Gb of long reads and 139.9 Gb of short reads were generated, with coverages of 42.3X and 45.8X, respectively. A draft genome (3.3 Gb) was de novo assembled; Chicago and Hi-C sequencing were used to improve chromosome-level scaffolding. The final assembly resulted in a smaller genome (3.06 Gb) with an N50 of 150.67 Mb, where the largest 48 scaffolds represent 94.6% completeness of the *P americana* genome. Among those scaffolds, the 25 largest exceeded the length threshold of 1 Mb, suggesting successful assembly of 25 chromosome-level scaffolds.

In silico prediction of putative allergens, based on amino acid sequence similarity relative to known allergens, identified 182 potentially allergenic hits in the *P americana* proteome. These protein hits were filtered according to % identity (threshold >50%), expression level (average transcripts per million >10), and the presence of potential epitopes, yielding a *P americana* allergome that comprised 135 components. Among these components, most previously reported *P americana* allergens across 13 groups were retrieved; the corresponding hits showed high % identities (90.74%-100.00%). No identical hits were observed for Per a 11.0101 or Per a 12.0101; however, highly conserved sequences (76.69% and 82.8%, respectively) were identified, suggesting the existence of potential isoallergens in groups 11 and 12. Moreover, groups 4 (lipocalin) and 8 (myosin) matched Pam_039016-T1 and Pam_063052-T1, with high identities of 98.91% and 99.52%, respectively.

112 of the 135 potential candidates were evaluated for allergenic potential. Most showed high similarity to allergens of arthropod origin such as those from cockroach, mosquito, and several mite species. Additionally, 20 and 19 Per a allergen candidates matched published Bla g allergens and Der f allergens with high similarity, respectively, indicating potential cross-reactivity between cockroach and mite allergens. Smaller numbers of the 112 candidates displayed similarity with allergens from fungi and other eukaryotes. Approximately 10% of the candidates showed some similarity with allergens from plants or sea animals, implying cross-reactivity between cockroach allergens and allergens from plant foods or seafood. Along with isoallergens from known groups, 30 novel allergen groups were predicted including cofilin, paramyosin, alpha-tubulin, cyclophilin, heat shock protein, porin 3, aldehyde dehydrogenase, ribosomal protein, enolase, and aldolase. Many newly predicted allergens belonged to three multigene families: glutathione-S transferases, alpha-tubulin, and cyclophilin. The high diversification in group 5 (glutathione-S transferases) emphasised that the 67% similarity cut-off for isoallergen assignment was arbitrary and only intended to serve as a guide. Two group 5 allergens, Per a 5.0101 and Per a 5.0102, shared only 18% identity and 33% similarity with the first identified glutathione-S transferases allergen Bla g 5 (O18598) in *Blattella germanica*, suggesting that criteria for determining isoallergens should be flexible when studying less conserved groups.

To consolidate our predictions, conventional methods for novel allergen identification (two-dimensional gel electrophoresis, immunoblotting, and mass spectrometry) were performed using *P americana* protein extracts and serum samples from allergy-positive patients. The well-annotated proteome served as a customised protein database that replaced the use of redundant public databases in identifying mass spectrometry hits, allowing 43 of 45 spots to be classified by allergen database searches. By integrating mass spectrometry results with in silico predictions, we selected several targets for experimental validation. The allergenicity of novel allergens: enolase (Per a 14), cytochrome C (Per a 15), cofilin (Per a 16), alpha-tubulin (Per a 17), cyclophilin (Per a 18), porin3 (Per a 19), and peroxiredoxin-6 (Per a 20), as well as a novel isoallergen in the tropomyosin group (Per a 7.02) were evaluated in allergy-positive patients using the ELISA. Exception for cytochrome C (Per a 15), the immunoglobulin E (IgE) reactivities of the other novel allergens were significantly higher in allergy-positive patients. The IgE sensitisation rates for these allergens exceeded 50%, suggesting that they can serve as novel major allergens in *P americana*. Cytochrome C (Per a 15) exhibited an IgE reactivity of 30% in allergy-positive patients.

Discussion

This study integrated genomic and transcriptomic analyses with proteomic techniques, including two-dimensional gel electrophoresis, mass spectrometry, and ELISA, to identify novel allergens in *Blattodea* species. The gene set annotated from our high-quality genome served as a customised protein database, which replaced the redundant public databases, in identifying mass spectrometry hits, allowing construction of a broader and more precise allergen spectrum. In total, 135 allergenic hits, comprising 23 previously published allergens and 112 in silico predicted allergens, were identified in the American cockroach. The allergenic features of multiple novel allergens or isoallergens (eg, alpha-tubulin, cyclophilin, cofilin, enolase, porin3, peroxiredoxin-6, and tropomyosin) were confirmed by mass spectrometry and ELISA.

The diagnosis of cockroach allergy primarily relies on skin prick test results or specific IgE sensitivity to cockroach allergens. A panel of purified recombinant cockroach allergens was previously established to facilitate component-resolved

diagnosis, which resolves the IgE specificity of each component and characterises patient sensitisation profiles. However, it is challenging to achieve diagnostic sensitivity comparable to that of natural cockroach extracts because of the incomplete allergen profile available, lack of immunodominant allergens, variability in allergen content across cockroach extracts, and heterogeneous patterns of IgE sensitivity among different patient groups. The incorporation of established allergen panels with our newly identified allergens (especially those belonging to novel groups) could potentially enhance IgE sensitivity in diagnostic tests, thereby improving the efficacy and accuracy of species-specific component-resolved diagnosis in certain populations. The absence of a standardised cockroach extract hinders routine clinical implementation of immunotherapy. Newly identified allergens with high IgE sensitisation rates (eg, enolase, alpha-tubulin, cyclophilin, cofilin, and tropomyosin) should be combined with current cockroach extracts to facilitate the standardisation of cockroach allergen extracts, enable risk stratification, and improve the management of individuals with complex sensitisation profiles.

The presence of contaminants, such as endotoxins and microbial proteins, can trigger unwanted immunological responses during allergen immunotherapy. In the future, the limitations of allergen extracts may be addressed by using purified allergens standardised for purity and biological activity. Pre-clinical trials involving Per a 9 and Per a 10 have been conducted. We anticipate that the novel cockroach allergens identified in the present study will become candidates for a purified allergen mixture in next-generation allergen immunotherapy, potentially reducing hypersensitive reactions triggered by *P americana*.

Funding

This study was supported by the Health and Medical Research Fund, Health Bureau, Hong Kong SAR Government (#07181266). The full report is available from the Health and Medical Research Fund website (https://rfs2.healthbureau.gov.hk).

Disclosure

The results of this research have been previously published in:

1. Wang L, Xiong Q, Saelim N, et al. Genome assembly and annotation of Periplaneta americana reveal a comprehensive cockroach allergen profile. Allergy 2023;78:1088-103.
2. Xiong Q, Wan AT, Liu X, et al. Comparative genomics reveals insights into the divergent evolution of astigmatic mites and household pest adaptations. Mol Biol Evol 2022;39:msac097.
3. Shi L, Xiong Q, Ao FK, et al. Comparative analysis of cysteine proteases reveals gene family evolution of the group 1 allergens in astigmatic mites. Clin Transl Allergy 2023;13:e12324.
4. Xiong Q, Liu X, Wan AT, et al. Genomic analysis reveals novel allergens of Blomia tropicalis. Allergol Int 2024;73:340-4.
5. Wan AT, Xiong Q, Xiao X, et al. Multi-omic analysis of *Tyrophagus putrescentiae* reveals insights into the allergen complexity of storage mites. Clin Exp Allergy 2024;54:77-81.

References

1. Do DC, Zhao Y, Gao P. Cockroach allergen exposure and risk of asthma. Allergy 2016;71:463-74.
2. Eggleston PA, Arruda LK. Ecology and elimination of cockroaches and allergens in the home. J Allergy Clin Immunol 2001;107(3 Suppl):S422-S429.

L-carnitine and cardiovascular disease: a Mendelian randomisation study (abridged secondary publication)

J Zhao *, S Burgess, BH Fan, CM Schooling

KEY MESSAGES

1. Our findings do not support a beneficial association between L-carnitine and cardiovascular disease or its risk factors but suggest potential harm.
2. Sex differences in cardiovascular effects of L-carnitine remain to be confirmed.
3. Our findings highlight concerns about dietary factors that increase carnitine levels (ie, red meat), with implications for dietary recommendations.

Hong Kong Med J 2025;31(Suppl 1):S41-4
HMRF project number: 16172921

[1] J Zhao, [2] S Burgess, [1] BH Fan, [1] CM Schooling

[1] *School of Public Health, The University of Hong Kong, Hong Kong SAR, China*
[2] *Cardiovascular Epidemiology Unit, Department of Public Health and Primary Care, University of Cambridge, United Kingdom*

* Principal applicant and corresponding author: janezhao@hku.hk

Introduction

Cardiovascular disease (CVD) is a leading cause of death worldwide. Effective interventions, especially daily dietary measures, are valuable for primary prevention and care. Red meat and its associated metabolites, such as trimethylamine-N-oxide (TMAO), are important for human and planetary health.[1] L-carnitine, the active form of dietary carnitine and a precursor to TMAO, is considered a target in CVD prevention and treatment. L-carnitine is abundant in animal products, especially red meat; it also serves as a nutrient supplement to increase endurance in athletes.

Evidence is contradictory regarding effectiveness and safety of L-carnitine in CVD. In a systematic review and meta-analysis of 13 controlled trials involving 3629 patients with acute myocardial infarction, L-carnitine is beneficial for angina but had no effect on heart failure or myocardial infarction outcomes.[2] These findings may be partly explained by short follow-up periods, variable L-carnitine dosage, and the inclusion of low-quality trials that lacked randomisation and blinding.[2] Additionally, there is speculation that dietary carnitine can accelerate atherosclerosis through metabolites from gut microbiota.[3]

In the absence of conclusive evidence from high-quality randomised controlled trails, naturally occurring L-carnitine-related genetic variants can be used to predict serum carnitine in Mendelian randomisation studies, thereby examining the role of L-carnitine without potentially harmful interventions.[4] Genetic variants are established at conception, making them less susceptible to confounders (eg, socioeconomic position) that can bias conventional observational studies. In this study, we used Mendelian randomisation to examine the associations of genetically predicted L-carnitine levels with CVD and its risk factors. We also assessed the association between red meat consumption and CVD by conducting a systematic review and meta-analysis of observational studies.

Methods

A two-sample Mendelian randomisation study was conducted based on large, well-established cohorts and consortia. Specifically, genetic proxies for L-carnitine were used in genome-wide association studies (GWAS) of CVD and its risk factors. The association of red meat consumption (including both unprocessed and processed red meat) with CVD was assessed through a systematic review and meta-analysis of observational studies.

Eight independent genome-wide significant single nucleotide polymorphisms (SNPs) associated with L-carnitine were identified from a GWAS meta-analysis involving 23 658 people of European ancestry, with adjustments for age, sex, and study-specific covariates.[5]

Primary outcome measures included fatal and non-fatal CVD events such as coronary artery disease (CAD), ischaemic stroke, heart failure, and atrial fibrillation (AF). Secondary outcome measures included type 2 diabetes, levels of glucose, glycated haemoglobin, and insulin, lipid profile (low- and high-density lipoprotein cholesterol, triglycerides, and apolipoprotein B), systolic and diastolic blood pressures, and body mass index, all of which constitute risk factors for CVD.

The Wald estimate (ie, the genetic association with CVD and its risk factors divided by the genetic association with L-carnitine) was calculated for

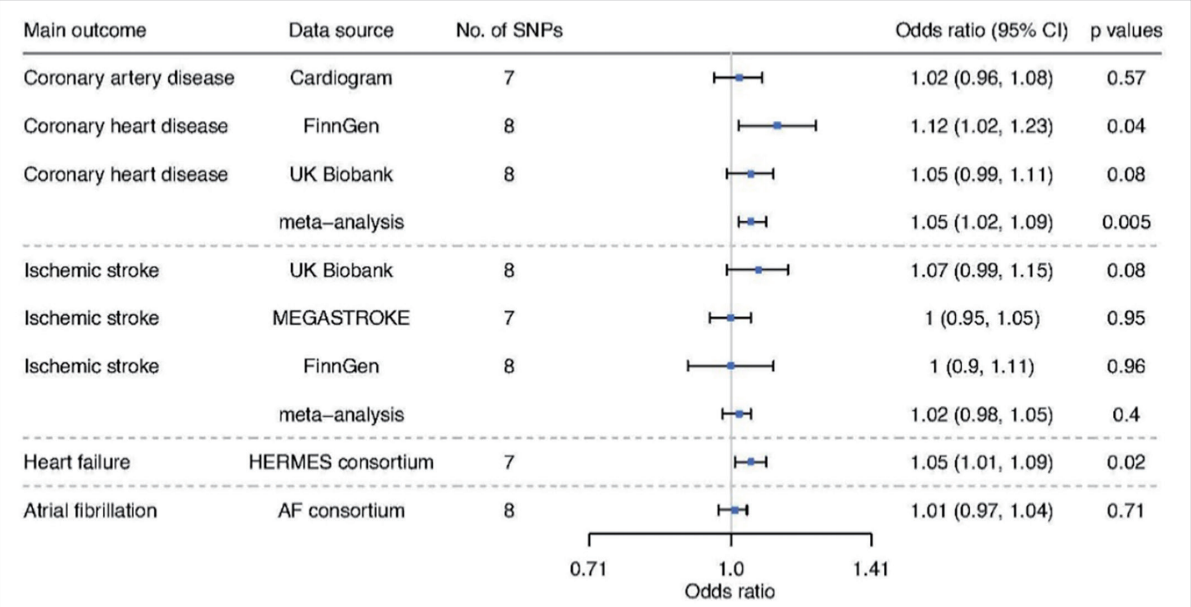

FIG 1. Odds ratios for cardiovascular diseases per standard deviation increase in genetically predicted L-carnitine level associated with eight independent genome-wide significant single nucleotide polymorphisms (SNPs)

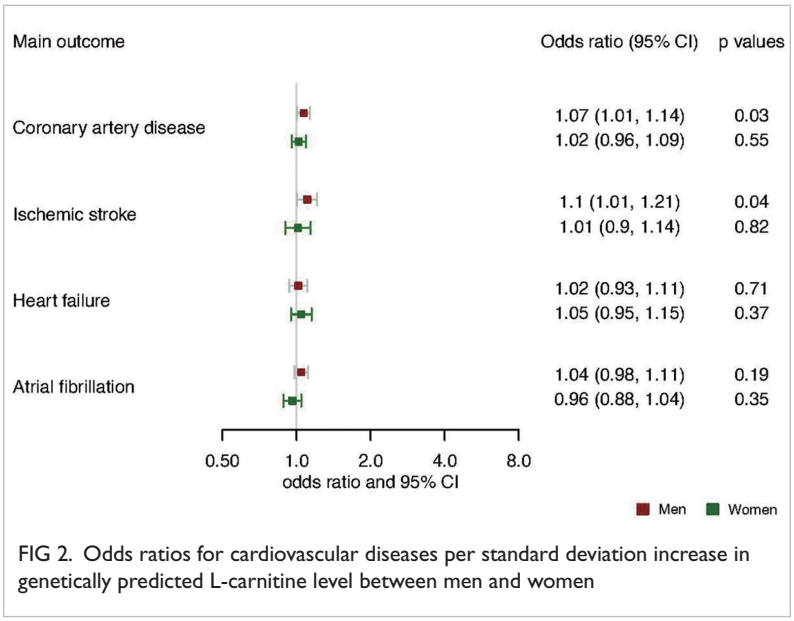

FIG 2. Odds ratios for cardiovascular diseases per standard deviation increase in genetically predicted L-carnitine level between men and women

each SNP. SNP-specific estimates were combined using inverse variance weighting with multiplicative random effects. Estimates from different data sources were meta-analysed. A Mendelian randomisation pleiotropy residual sum and outlier analysis, which uses the 'leave-one-out' approach, was conducted to identify outliers and provide a corrected estimate after outlier removal. The adjusted estimates served as the primary results if outliers were detected; otherwise, the inverse variance–weighted estimates were used. The analysis was repeated after sex stratification, with a heterogeneity test to assess differences between estimates.

PubMed, Web of Science, Embase, and the Cochrane Library were searched for studies regarding associations between red meat consumption and CVD. The search terms included synonyms and combinations of terms for red meat and CVD. Only observational studies (cohort studies, cross-sectional, and case-control) with available full texts were included. When multiple studies analysed the same population, only the most recent study was used. Relative risks and 95% confidence intervals were calculated using inverse variance-weighted meta-analysis. Heterogeneity between studies was evaluated using I^2. High heterogeneity was defined using thresholds of I^2 >50% and P values of <0.10; in these cases, a random-effects model was used. Otherwise, a fixed-effects model was used. Subgroup analyses according to sex and region (Western and Eastern populations) also were conducted.

Results

Each standard deviation increase in genetically predicted L-carnitine level was associated with a higher risk of CAD (odds ratio [OR]=1.05) and heart failure (OR=1.05); however, it was not associated with ischaemic stroke (OR=1.02) or AF (OR=1.01) [Fig 1]. Specifically, it was associated with a higher risk of CAD in men (OR=1.07) but not in women (OR=1.02), although this sex difference was not significant (P=0.31) [Fig 2].

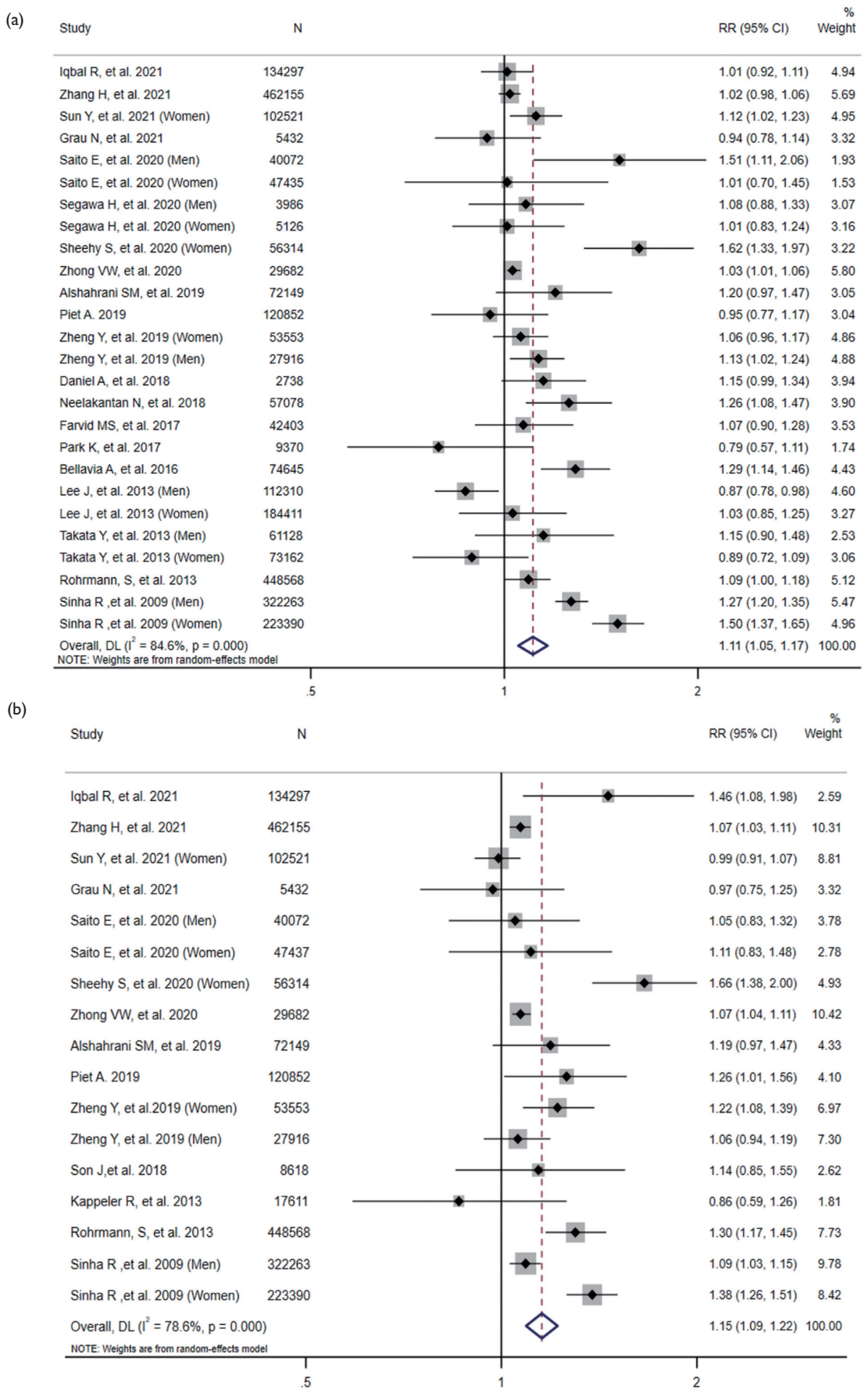

FIG 3. Meta-analysis of the associations of (a) unprocessed and (b) processed red meat consumption with cardiovascular disease risk

Each standard deviation increase in genetically predicted L-carnitine level was associated with higher triglyceride levels (effect size was 0.04 overall, 0.05 in men, and 0.03 in women; no significant sex difference) and lower high-density lipoprotein cholesterol levels (effect size was -0.02 overall, -0.04 in men, and 0.004 in women [P=0.88]). It also was associated with a higher risk of diabetes (P=0.04) but not with other glycaemic traits (levels of glucose, glycated haemoglobin, or insulin).

Of the 5743 studies identified, 22 met the inclusion criteria for meta-analysis. Higher red meat consumption was associated with increased CVD risk (relative risk was 1.11 for unprocessed red meat and 1.15 for processed red meat) [Fig 3]. There were no significant differences according to sex or region.

Discussion

Our Mendelian randomisation study indicated that L-carnitine does not have beneficial effects on CVD or its risk factors and instead may be harmful. The meta-analysis of observational studies suggested that higher red meat consumption is associated with increased CVD risk.

Endogenous L-carnitine may not fully reflect the effects of exogenous carnitine supplementation. However, L-carnitine can be readily obtained from dietary sources, and the highest content is present in red meat. L-carnitine levels rise after red meat consumption, and higher red meat consumption is associated with increased CVD risk. The absence of detectable sex differences might be due to the limited number of studies that examine men and women separately. The lack of regional differences could reflect lower levels of red meat consumption in Eastern populations or the effects of confounders, particularly socio-economic status, which strongly influences both diet and health outcomes.

Our study had several limitations. First, although Mendelian randomisation estimates are less susceptible to confounding than conventional observational studies, they are less precise because genetic variants only explain a small proportion of the variance in exposure. Replication in larger samples, especially for nominal associations, is therefore warranted. Second, the role of L-carnitine might be influenced by interactions with microbiota, but information about microbiota is not available in UK Biobank data. Third, the genetic instruments for L-carnitine were derived from GWAS of metabolites; replication via GWAS focused on L-carnitine is needed. Fourth, observational studies included in the meta-analysis are susceptible to confounding and selection biases. Finally, few studies provided subgroup analyses stratified by sex, making it difficult to identify sex-specific differences. Future studies should explore the benefits of lower red meat consumption on CVD risk through randomised controlled trials. Our findings highlight concerns about dietary factors that increase L-carnitine levels, such as red meat, with implications for dietary recommendations. Sex differences in the effects of L-carnitine remain to be confirmed, and the underlying mechanisms warrant further investigation.

Conclusion

Our findings do not support a beneficial association between L-carnitine and CVD or its risk factors but suggest potential harm. Lower red meat consumption is recommended; this also contributes to an environmentally friendly lifestyle.

Funding

This study was supported by the Health and Medical Research Fund, Health Bureau, Hong Kong SAR Government (#16172921). The full report is available from the Health and Medical Research Fund website (https://rfs2.healthbureau.gov.hk).

Disclosure

The results of this research have been previously published in:

1. Zhao JV, Burgess S, Fan B, et al. L-carnitine, a friend or foe for cardiovascular disease? A Mendelian randomization study. BMC Med 2022;20:272.
2. Shi W, Huang X, Schooling CM, Zhao JV. Red meat consumption, cardiovascular diseases, and diabetes: a systematic review and meta-analysis. Eur Heart J 2023;44:2626-35.

References

1. Abbasi J. TMAO and Heart Disease: The new red meat Risk? JAMA 2019;321:2149-51.
2. DiNicolantonio JJ, Lavie CJ, Fares H, Menezes AR, O'Keefe JH. L-carnitine in the secondary prevention of cardiovascular disease: systematic review and meta-analysis. Mayo Clin Proceed 2013;88:544-51.
3. Johri AM, Heyland DK, Hetu MF, Crawford B, Spence JD. Carnitine therapy for the treatment of metabolic syndrome and cardiovascular disease: evidence and controversies. Nutr Metab Cardiovasc Dis 2014;24:808-14.
4. Lawlor DA, Harbord RM, Sterne JA, Timpson N, Davey Smith G. Mendelian randomization: using genes as instruments for making causal inferences in epidemiology. Stat Med 2008;27:1133-63.
5. Lotta LA, Pietzner M, Stewart ID, et al. A cross-platform approach identifies genetic regulators of human metabolism and health. Nat Genetics 2021;53:54-64.

Semen metagenomics and spent culture media in patients undergoing conventional in vitro fertilisation: abridged secondary publication

MBW Leung, DYL Chan *, EKL Fok, HCH Yim, X Jiang, TC Li

KEY MESSAGES

1. Vertical transmission of microbes was identified in 82.5% of spent embryo culture medium samples; semen was the primary source of contamination.
2. Increased abundances of *Staphylococcus* and *Streptococcus anginosus* were associated with reduced sperm count and total motility, respectively.
3. Microbiomes in spent embryo culture medium and seminal fluid were not associated with assisted reproductive technology treatment outcomes including fertilisation rates, embryo development, number of available embryos, clinical pregnancy rates, miscarriage rates, and live birth rates.

Hong Kong Med J 2025;31(Suppl 1):S45-7
HMRF project number: 19181162

[1] MBW Leung, [1] DYL Chan, [2] EKL Fok, [3] HCH Yim, [3] X Jiang, [1] TC Li

[1] *Department of Obstetrics and Gynaecology, Prince of Wales Hospital, The Chinese University of Hong Kong, Hong Kong SAR, China*
[2] *School of Biomedical Sciences, The Chinese University of Hong Kong, Hong Kong SAR, China*
[3] *Microbiome Research Centre, The University of New South Wales, Australia*

* Principal applicant and corresponding author: drdcyl16@cuhk.edu.hk

Introduction

In conventional in vitro fertilisation (IVF), contamination of embryo culture occurs in 0.38% to 8% of cases. The true prevalence of microbial colonisation is probably underestimated primarily due to the lack of evidence; most cases are only identified when turbidity or bacterial growth is observed. The source of contamination in culture media is usually unknown, but microbes are believed to predominantly originate from seminal fluids and are vertically transmitted to culture media during fertilisation. Bacteria have also been detected in follicular fluids. However, the association between embryo culture media contamination and assisted reproductive technology (ART) outcomes remains unclear. We hypothesised that spent embryo culture media (SECM) is not strictly sterile and that microbes may be vertically transmitted from seminal and follicular fluids into culture media during ART treatment. This study aimed to determine the prevalence of vertical microbial transmission into embryo culture media and the associations between ART outcomes and the microbiomes of SECM, semen, and follicular fluid.

Methods

Infertility patients seeking ART treatment at the Prince of Wales Hospital, Hong Kong, were invited to participate. Follicular fluid from the largest follicle was aspirated from each ovary, transferred into a sterile test tube, and centrifuged to remove debris. Semen samples were prepared for insemination using standard density gradient centrifugation; the supernatant seminal fluid was stored at -80°C. Fertilised embryos were transferred into a new culture dish containing fresh drops (25 mL) of embryo culture media for further culture. SECM samples were stored at -80°C for microbiome analysis. Unused embryo culture medium drops served as negative controls. All samples were subjected to DNA extraction, and standardised samples were prepared for sequencing. Bioinformatics and statistical analyses were conducted.

Results and discussion

Of 196 couples recruited, 88 were excluded and 108 were included in the analysis. The mean ages of male and female participants were 36.0 and 34.8 years, with mean body mass indices of 23.8 and 22.2 kg/m^2, respectively (Table). The 16S rRNA amplicon analysis generated a median of 43 800 reads per sample. After decontamination, 2189 unique amplicon sequence variants were identified: 457 (21.9%) were exclusively detected in SECM, 464 (26.2%) were exclusively detected in semen, and 627 (31.5%) were exclusively detected in follicular fluids; 97 taxa (4.4%) were shared among all specimen types.

Vertical transmission of microbes was identified in 82.5% of SECM samples; semen was the primary source of contamination. Firmicutes, Proteobacteria, Bacteroidetes, and Actinobacteria were the four dominant phyla (Fig). At the genus level, *Lactobacillus*, *Streptococcus*, *Staphylococcus*,

TABLE . Characteristics of participants (n=108 pairs)

Characteristic	Value*
Age, y	
Women	34.8±3.1
Men	36.0 (36.3-38.4)
Body mass index, kg/m²	
Women	22.2 (22.3-23.8)
Men	23.8 (23.2-25.3)
Cigarette smokers	
Women (n=61)	5 (8.2)
Men (n=61)	14 (23.0)
Alcohol consumers	
Women (n=61)	7 (11.5)
Men (n=61)	10 (16.4)
Aetiology of infertility (n=61)	
Tubal occlusion	19 (31.2)
Pelvic adhesions	20 (32.8)
Endometriosis	17 (27.9)
Uterine factor	5 (8.2)
Male factor	52 (85.2)
Ovulatory disorders (including polycystic ovarian syndrome)	9 (14.8)
Coital dysfunction	3 (4.9)
Idiopathic infertility	3 (4.9)

* Data are presented as mean ± standard deviation, median (95% confidence interval), or No. (%) of participants

Bacillus, *Prevotella*, and other microbes were detected in SECM samples.

In seminal fluid, microbial taxa detected in normozoospermic men were comparable to those in men with defective semen parameters. However, increased abundances of *Staphylococcus* and *Streptococcus anginosus* were associated with reduced sperm count and total motility, respectively (P<0.001). In follicular fluid, the relative abundance of *Porphyromonas* was associated with anovulation (P<0.001); *Neisseria* was more abundant in women with uterine factor infertility than in women with other causes of infertility (P<0.01). The relative abundance of *Facklamia* was associated with unexplained infertility (P<0.01). Despite these findings, the microbiomes of SECM, seminal fluid, and follicular fluid were not associated with ART outcomes including fertilisation rates, embryo development, number of available embryos, and clinical pregnancy rates.

Conclusion

Embryo culture media is primarily contaminated by semen and, to a lesser extent, by follicular fluid. Strong associations were observed between specific microbial taxa in semen and sperm quality, as well as between follicular fluid microbiomes and the aetiology of infertility in women. However, the microbiomes of SECM, semen, and follicular fluid were not associated with ART treatment outcomes.

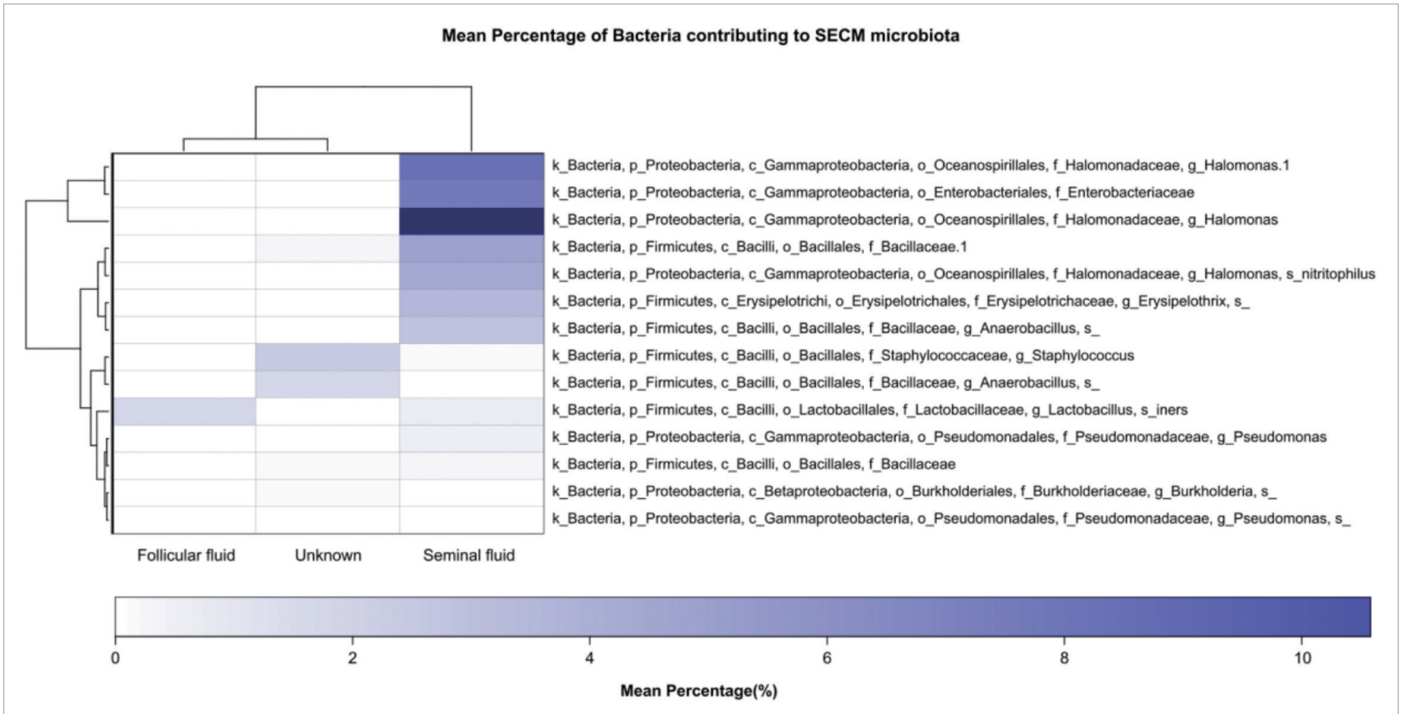

FIG. Mean percentages of bacteria contributing to spent embryo culture media microbiota

Funding

This study was supported by the Health and Medical Research Fund, Health Bureau, Hong Kong SAR Government (#19181162). The full report is available from the Health and Medical Research Fund website (https://rfs2.healthbureau.gov.hk).

Disclosure

The results of this research have been previously published in:

1. Alqawasmeh O, Fok E, Yim H, Li T, Chung J, Chan D. The microbiome and male infertility: looking into the past to move forward. Hum Fertil (Camb) 2023;26:450-62.

2. Alqawasmeh OAM, Jiang XT, Cong L, et al. Vertical transmission of microbiomes into embryo culture media and its association with assisted reproductive outcomes. Reprod BioMed Online 2024;49:103977.

Published by the Hong Kong Academy of Medicine Press for the Government of the Hong Kong Special Administrative Region. The opinions expressed in the *Hong Kong Medical Journal* and its supplements are those of the authors and do not reflect the official policies of the Hong Kong Academy of Medicine, the Hong Kong Medical Association, the institutions to which the authors are affiliated, or those of the publisher.